Geochemistry Geophysics Geosystems G3

Article
Volume 13, Number 10
30 October 2012
Q10019, doi:10.1029/2012GC004233
ISSN: 1525-2027

Published by AGU and the Geochemical Society

Tracing mantle sources and Samoan influence in the northwestern Lau back-arc basin

Marion L. Lytle and Katherine A. Kelley
Graduate School of Oceanography, University of Rhode Island, South Ferry Road, Narragansett, Rhode Island 02882, USA (lytleml@gso.uri.edu)

Erik H. Hauri
Department of Terrestrial Magnetism, Carnegie Institute of Washington, 5241 Broad Branch Road NW, Washington, D. C. 20008, USA

James B. Gill and Dominic Papia
Earth and Planetary Sciences Department, University of California, Santa Cruz, California 95064, USA

Richard J. Arculus
Research School of Earth Sciences, Australian National University, Canberra, ACT 0200, Australia

[1] Helium isotopes are commonly used as a diagnostic fingerprint of Samoan mantle in the northern Lau Basin, but the extent of input from Samoan sources can only be clearly resolved by coupling $^{3}He/^{4}He$ with other geochemical tracers such as trace elements and other isotope systems. We present new major element, dissolved volatile (H_2O, CO_2, S, Cl, F), trace element, and Sr-Nd-Pb-Hf isotope data for new samples from the NW Lau Basin from five distinct regions (Rochambeau Rifts (RR), Northwest Lau Spreading Center (NWLSC), Peggy Ridge (PR), Lau Extensional Transform Zone (LETZ), and Central Lau Spreading Center (CLSC)) that range from distinctively elevated to normal mid-ocean ridge basalt $^{3}He/^{4}He$. Helium isotopes variations are not correlated with radiogenic isotopes or trace element abundances. Our new data suggest two-component mixing of MORB-like mantle with an enriched mantle source, similar to Samoa, although consideration of a complete regional data set suggests there may be other sources of heterogeneity in the mantle beneath NW Lau. Models of mantle potential temperature (T_p) and primary melt equilibration temperatures indicate similar T_p of ~1400°C for NW Lau, suggesting no strong temperature gradient. The pressure of melt equilibration deepens toward the north (~1.1–1.2 GPa at PR, LETZ, CLSC; ~1.3–1.4 GPa at RR, NWLSC), consistent with melting mantle of a constant T_p but variable H_2O content. Samoan and MORB-like sources are clearly present beneath the NW Lau basin, but geochemical diversity among the existing data suggest that more than two mantle sources may contribute to mantle enrichment beneath NW Lau.

Components: 13,000 words, 10 figures.

Keywords: Lau back-arc basin; Samoan plume; basalt; hot spot; mantle heterogeneity.

Index Terms: 1038 Geochemistry: Mantle processes (3621); 1065 Geochemistry: Major and trace element geochemistry; 3001 Marine Geology and Geophysics: Back-arc basin processes.

Received 14 May 2012; **Revised** 21 September 2012; **Accepted** 25 September 2012; **Published** 30 October 2012.

Lytle, M. L., K. A. Kelley, E. H. Hauri, J. B. Gill, D. Papia, and R. J. Arculus (2012), Tracing mantle sources and Samoan influence in the northwestern Lau back-arc basin, *Geochem. Geophys. Geosyst.*, *13*, Q10019, doi:10.1029/2012GC004233.

1. Introduction

[2] Tracing long-term movements of the Earth's mantle through direct observation of the Earth itself is tremendously difficult, given the enormous contrast in time scales over which tectonic/dynamic motions occur relative to the brief periods over which observations may be made. Studies of shear wave splitting provide characterizations of mantle anisotropy and flow, as olivine *a*-axes align with mantle flow vectors [e.g., *Silver and Chan*, 1991; *Zhang and Karato*, 1995]. Beneath volcanic arcs, shear wave splitting studies suggest a range of potential vectors, from arc-normal to arc-parallel [e.g., *Russo and Silver*, 1994; *Smith et al.*, 2001; *Conder and Wiens*, 2007], challenging conventional ideas about the coupling of plate and mantle wedge flow. Geochemistry provides another tool to image mantle flow, particularly in places where mantle sources of contrasting geochemical characteristics are juxtaposed.

[3] Using geochemistry to trace mantle flow has been successfully applied in the Mariana subduction system, where four primary contributions to the mantle source have been identified using Nb/Ta and Ta/Yb ratios, including a depleted mantle asthenosphere and enriched lithosphere that are modified by at least two distinct subduction-derived components [*Pearce et al.*, 2005]. Additionally, while Pb isotopes distinguish two different mantle domains (Pacific and Indian) in the southwest Pacific, Pb mobility during subduction makes tracing the flow of these distinct mantle domains challenging [see *Heyworth et al.*, 2011]. The use of less mobile Hf-Nd isotopes provides alternative geochemical tracers of the two mantle domains, showing the influx of the Indian mantle into the Fiji Islands and the N. Fiji and Lau Basins [*Pearce et al.*, 2007].

[4] The Lau Basin has been a particular focal point for efforts to trace mantle domains and movements using geochemistry. Extensive work at the Eastern Lau Spreading Center (ELSC), has shown a regional connection between decreasing subduction influence in the back-arc with increasing distance from the Tonga Arc [*Escrig et al.*, 2009]. The ELSC also shows evidence of mixing between a number of mantle components, including Indian-like mantle and an enriched mid-ocean ridge basalt (MORB) mantle, with materials derived from the subducted slab [*Bézos et al.*, 2009; *Escrig et al.*, 2009]. The NW Lau Basin, on the other hand, comprises several spreading centers and rift zones that are located far west of the active subduction zone and are not likely to be influenced by modern subduction. The elevated He isotopic signature of the nearby Samoan Plume has long been viewed as a diagnostic tracer of enriched Samoan mantle, and following this rationale, basalts erupted in the NW Lau Basin with $^{3}He/^{4}He$ ratios higher than MORB suggest influence from a Samoa-like source in the mantle beneath NW Lau [e.g., *Hawkins and Melchior*, 1985; *Poreda*, 1985; *Wright and White*, 1987; *Farley et al.*, 1992; *Poreda and Craig*, 1992; *Lupton et al.*, 2009]. Reliance on a singular geochemical tracer as evidence of the regional movement of Samoan mantle however, leaves room for doubt about the origin of the elevated $^{3}He/^{4}He$ isotope ratios in the Lau Basin, particularly since other western Pacific back-arc basins have similarly elevated $^{3}He/^{4}He$ in the absence of a known nearby mantle plume (e.g., Manus basin [*Shaw et al.*, 2004]). Do the Lau helium isotopes correlate with other geochemical signatures of Samoan mantle? Is there corroborative evidence, such as elevated mantle temperature, of hot spot influence beneath NW Lau? These questions must be addressed before the presence or scale of Samoan mantle migration into the NW Lau Basin can be clearly resolved.

[5] With this work, we aim to address these outstanding questions with new geochemical data for major and trace elements, dissolved volatiles, and radiogenic isotopes for a suite of glasses from a high-density sampling of spreading centers and rift zones in the NW Lau Basin. These samples have been previously analyzed for $^{3}He/^{4}He$ ratios [*Lupton et al.*, 2009], and our work thus adds essential geochemical constraints on the genesis of NW Lau magmas that we use to test the identity of the enriched He signature, both through trace element/isotopic systematics and their relationships (or lack thereof) to He isotopes, and through petrologic modeling of mantle melting conditions beneath NW Lau spreading centers. We show that, surprisingly, He isotopes do not correlate with trace element or isotopic signatures in NW Lau, and that a portion of the mantle signature in this region, though elevated in $^{3}He/^{4}He$, is otherwise uncharacteristic of Samoa in its trace element and isotopic composition. Moreover, mantle temperature in the region, although high, does not decrease

toward the south as it would if hot mantle were infiltrating from the north. We explore the consequences of these observations for models of mantle flow in this complex region, and present alternative hypotheses that could explain the data.

1.1. Tectonic Setting

[6] The Tonga-Lau system is an oceanic subduction zone in the southwest Pacific, where the Pacific Plate subducts beneath the Indo-Australian Plate (Figure 1). Behind the Tonga Arc, back-arc spreading initiated at ~6 Ma in the Lau Basin [*Taylor et al.*, 1996], which is a V-shaped basin with several actively spreading segments that impinge on the Tonga Arc toward the south. The rates of both plate convergence and back-arc spreading are highest at the north end of the subduction zone [*Hawkins*, 1995], which exhibits the fastest back-arc opening on Earth, spreading at a rate of 160 mm/yr, decreasing southwards to rates of 60 mm/yr [e.g., *Bevis et al.*, 1995; *Taylor et al.*, 1996] (see Figure 1). At the northern end of the Tonga Arc, the plate boundary bends 90° and the Pacific Plate ceases to subduct. This northern boundary of the system is the Vitiaz Lineament, interpreted to be a paleo-subduction zone that is now a transform boundary separating the Pacific and Indo-Australian plates [*Hawkins*, 1995], and is likely the locus of a tear in the Pacific Plate at depth [*Millen and Hamburger*, 1998]. To the northeast of Tonga lies Samoa (Figure 1), an ocean island hot spot with an age-progressive volcanic chain on the Pacific Plate [e.g., *Hart et al.*, 2004; *Koppers et al.*, 2008] that may be the surface expression of a deep-rooted mantle plume [e.g., *Montelli et al.*, 2004; *Jackson et al.*, 2007a].

1.2. Prior Work

[7] Several previous studies have attempted to assess the nature and extent of interactions between Samoan mantle and the Lau Basin through a tear in the Pacific Plate at the northern end of the Tonga/Lau system. *Gill and Whelan* [1989] first used Nd isotopes to show that enriched Ocean Island basalt (OIB) source mantle had reached Fiji by 3 Ma. *Poreda and Craig* [1992] first analyzed He and Sr isotopes in a small population of samples from the Rochambeau Bank (RB), a shallow submarine volcanic center near the Vitiaz Lineament (note that RB is distinct from the region of rifting, Rochambeau Rifts (RR), immediately to the east; Figures 1b and 1c). They showed that some samples from RB have elevated $^{3}He/^{4}He$ ratios (up to 22 R_a; where $R = {}^{3}He/^{4}He$ and $R_a = R_{air} = 1.39 * 10^{-6}$) and enriched Sr isotopic signatures relative to lavas from further south in the Lau Basin that are more typical of normal mid-ocean ridges ($^{3}He/^{4}He$ = 8–10 R_a; Peggy Ridge (PR), Central Lau Spreading Center (CLSC)). Because Samoan lavas can have very high $^{3}He/^{4}He$ ratios (up to 33.8 Ra [*Jackson et al.*, 2007b]) and very radiogenic $^{87}Sr/^{86}Sr$, the elevated He and Sr isotope ratios at RB were used as evidence of mixing between enriched Samoan mantle, which was proposed to be drawn into the Lau Basin by mantle flow influenced by crustal extension at the spreading centers, and "ambient" depleted mantle beneath RB [*Poreda and Craig*, 1992].

[8] Further work [e.g., *Hilton et al.*, 1993; *Turner and Hawkesworth*, 1998; *Lupton et al.*, 2009] has refined these initial hypotheses, although until very recently, none have involved a focused regional survey and comprehensive sampling of spreading centers in northwestern Lau. *Turner and Hawkesworth* [1998] reviewed data for the northern Lau Basin, including Niuafo'ou island (NF) and the Mangatolu Triple Junction (MTJ; Figure 1b), concluding that elevated He isotope ratios were sufficient evidence for the presence of Samoan mantle beneath the Lau Basin despite radiogenic isotope signatures that were not conclusively related to Samoa. *Lupton et al.* [2009] analyzed $^{3}He/^{4}He$ ratios of 41 new glass samples from a comprehensive survey and sampling of spreading centers in the NW Lau Basin (a subset of the samples in this study). Their study found that all lavas north of the PR had $^{3}He/^{4}He$ ratios higher than MORB but, surprisingly, found no clear correlation between $^{3}He/^{4}He$ ratios and latitude or ridge morphology. Recent work by *Tian et al.* [2011] reported trace element and Sr-Nd radiogenic isotope data for northern Lau Basin samples from RB, PR, MTJ, and NF, including the RB samples from *Poreda and Craig* [1992]. Their results suggested a geochemically heterogeneous mantle source with both a subduction signature (in the east) and an enriched mantle source signature (in the west) from two Samoa-like end-members. *Hahm et al.* [2012] built upon this data set by analyzing volatiles and noble gases in these samples. Their results suggest hot spot influence in the NW Lau magmas. Moreover, further analyses of samples from the *Lupton et al.* [2009] study were conducted for Ne isotopes [*Lupton et al.*, 2012] and chalcophile elements [*Jenner et al.*, 2012]. The Ne isotopes correlate with $^{3}He/^{4}He$, providing additional evidence for influence from the Samoan Plume [*Lupton et al.*, 2012]. The chalcophile element data showed Cu

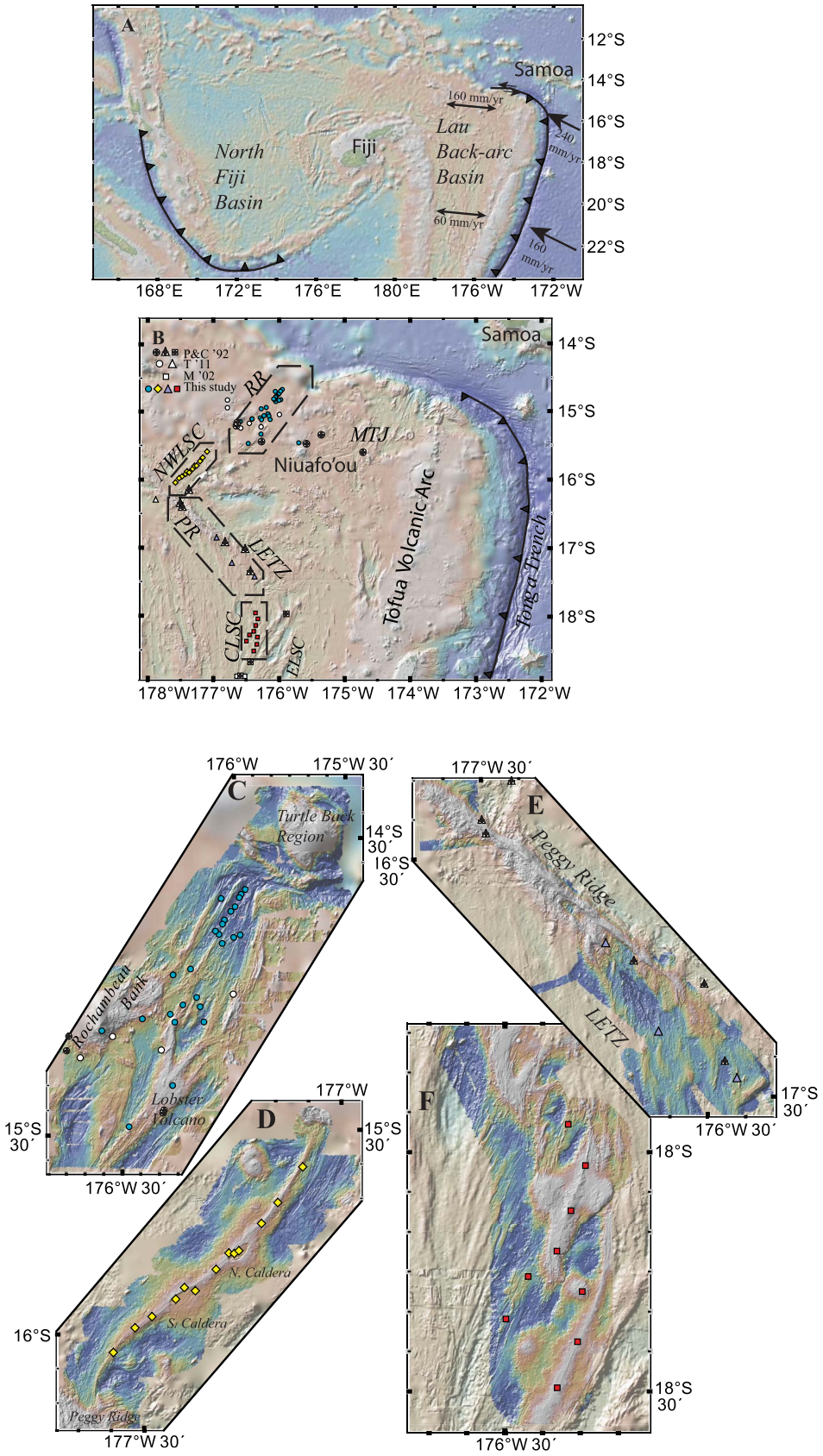
A
Samoa
160 mm/yr
240 mm/yr
North Fiji Basin
Fiji
Lau Back-arc Basin
60 mm/yr
160 mm/yr
12°S
14°S
16°S
18°S
20°S
22°S
168°E
172°E
176°E
180°E
176°W
172°W
B
P&C '92
T '11
M '02
This study
Samoa
RR
MTJ
Niuafo'ou
NWLSC
PR
LETZ
CLSC
ELSC
Tofua Volcanic Arc
Tonga Trench
14°S
15°S
16°S
17°S
18°S
178°W
177°W
176°W
175°W
174°W
173°W
172°W
C
Turtle Back Region
Rochambeau Bank
Lobster Volcano
176°W
175°W 30´
14°S 30´
16°S 30´
15°S 30´
176°W 30´
D
N. Caldera
S. Caldera
Peggy Ridge
177°W
16°S
15°S 30´
177°W 30´
E
Peggy Ridge
LETZ
177°W 30´
17°S 30´
176°W 30´
F
18°S
18°S 30´
176°W 30´

Figure 1

and Ag enrichment uncharacteristic of MORB or Samoan sources, suggesting the presence of an additional high-Cu mantle source in the region. The lack of a simple trend of decreasing $^3He/^4He$ in NW Lau with distance from the northern plate boundary [*Lupton et al.*, 2009], coupled with a scarcity of supportive data for these samples (e.g., major, trace, volatile elements or radiogenic isotope ratios), raises questions about the simple hypothesis of plume migration into the Lau Basin mantle. With the present study, we provide new data to accompany the He isotopes for these samples and use these data to assess the identities of mantle sources beneath the Lau Basin and the consequences for interpretations of mantle flow in this region based on lava geochemistry.

2. Samples and Methods

[9] The basaltic glass samples reported here are new samples from the Northern Lau Basin that were collected from 63 bottom dredges during voyage SS07/2008 of the R/V *Southern Surveyor*. Sample locations and rock descriptions including phenocryst information are given in auxiliary material Table S1 in Text S2.[1] The samples were analyzed for major elements by electron microprobe, trace elements by laser ablation and solution inductively coupled plasma mass spectrometry, volatiles by secondary ionization mass spectrometry, and radiogenic isotopes by multicollector inductively coupled plasma mass spectrometry (see auxiliary material for more detailed information on sample selection and analysis methods).

3. Results

3.1. Effects of Degassing

[10] As magma ascends from the mantle to the surface, dissolved volatiles will exsolve into a vapor phase at low pressures, resulting in volatile loss from the melt. Major volatile species (e.g., H_2O, CO_2) have different vapor/melt solubilites, enabling an assessment of volatile loss from each glass. Carbon dioxide has lower solubility in silicate melt at low pressure and is expected to begin degassing before H_2O [*Dixon and Stolper*, 1995], and the mixed CO_2-H_2O content of a glass reflects the minimum pressure of final equilibration of vapor-melt if the latter was volatile-saturated. Figure 2a shows CO_2 versus H_2O in the glasses from NW Lau, which indicate vapor saturation at pressures of 200–400 bars. Model degassing paths show that CO_2 is more sensitive to the early stages of degassing, and that H_2O loss is not significant until most CO_2 has been removed from the melt [*Newman and Lowenstern*, 2002]. Based on this analysis, most glasses have likely lost variable amounts of CO_2, but H_2O concentrations are relatively unmodified from the original magmatic values, with the exception of three andesite-composition glasses from NWLSC that have lost virtually all of their CO_2. Figure 2b compares the calculated pressure at H_2O-CO_2 saturation with the hydrostatic pressure at the mean collection depth of each sample. Most samples are found to be vapor-oversaturated or saturated at the pressure of collection, which is typical of mid-ocean ridge basalts and reflects relatively fast transport and eruption of magma from mid-crustal depths [*Danyushevsky et al.*, 1993].

3.2. Effects of Crystallization

[11] Assessing the extent of H_2O degassing is important because H_2O influences magmatic crystallization and the liquid line of descent (LLD). Water suppresses plagioclase and clinopyroxene crystallization [e.g., *Sisson and Grove*, 1993a, 1993b] and its effects can be seen in the major element systematics of the NW Lau basalts. The basalts can be segregated into two major groups on the basis

[1]Auxiliary materials are available in the HTML. doi:10.1029/2012GC004233.

Figure 1. (a) Regional map of the southwest Pacific, focusing on the Fiji and Samoa region. The Lau Back-arc Basin is opening behind the Tonga-Kermadec arc at a rate of 60–160 mm/yr, increasing northward to the plate boundary while the Pacific Plate subducts at a rate of 160–240 mm/yr [*Bevis et al.*, 1995]. (b) Detailed map of the northern Lau Basin, showing samples from Rochambeau Rifts (RR; circles), Northwest Lau Spreading Center (NWLSC; diamonds), Peggy Ridge/Lau Extensional Transform Zone (PR/LETZ; triangles), and the Central Lau Spreading Center (CLSC; squares). The Eastern Lau Spreading Center (ELSC), Mangatolu Triple Junction (MTJ), and Niuafo'ou island are identified for reference. The shaded symbols are samples from this study, the open squares are *Melson et al.* [2002], the open circles and triangles are from *Tian et al.* [2011], and the crossed symbols are from *Poreda and Craig* [1992]. The dashed lines outline the regions shown on Figures 1c–1f. Basemaps in Figures 1a and 1b were created using GeoMapApp (http://www.geomapapp.org) [*Ryan et al.*, 2009]. (c–f) Swath bathymetry maps and sample locations for the four main regions of this study: RR, NWLSC, PR/LETZ, and CLSC. High-resolution bathymetry was collected in 2008 by R/V Southern Surveyor using an EM300 multibeam bathymetry system.

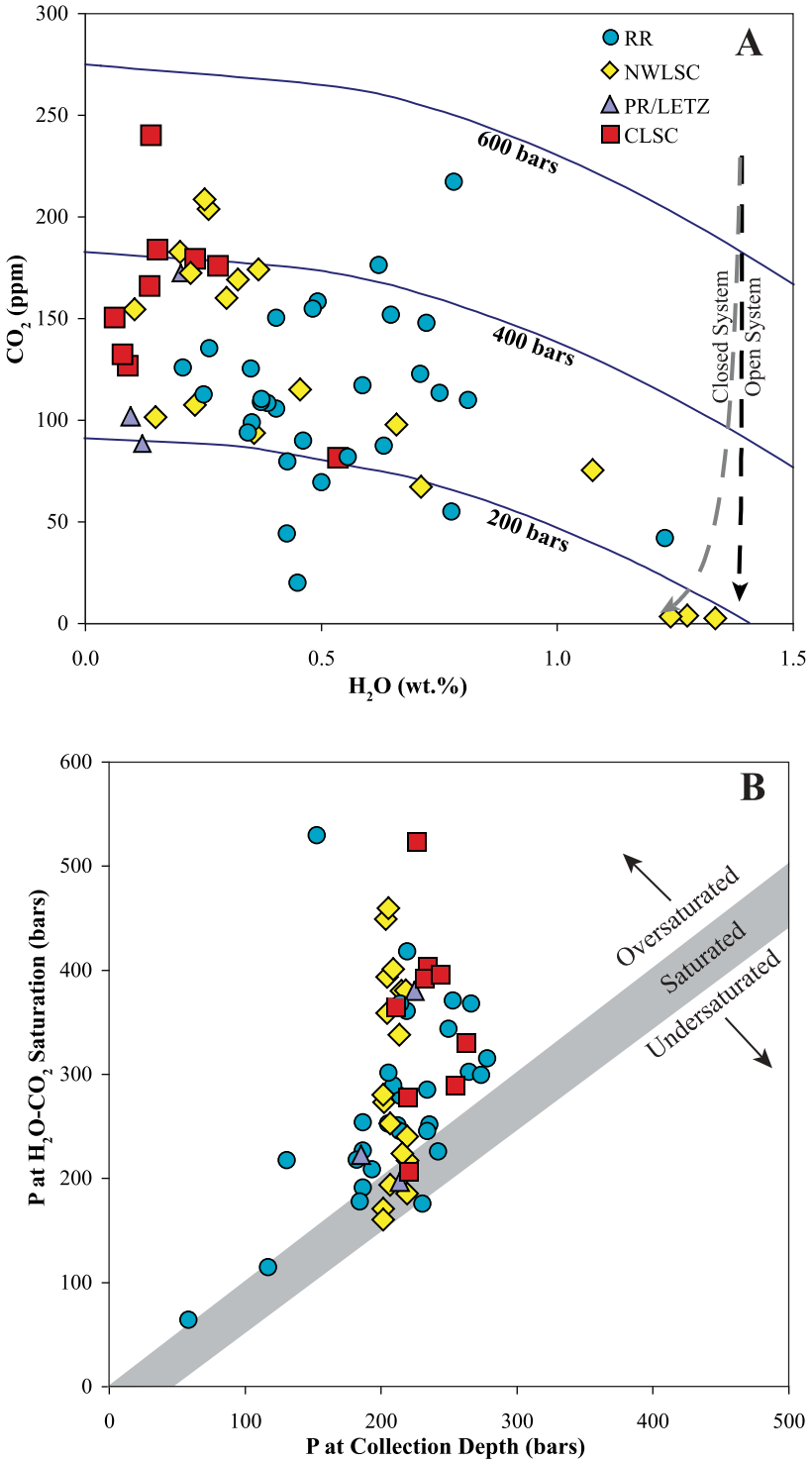

Figure 2. (a) Plot of CO_2 versus H_2O, showing samples from Rochambeau Rifts (RR; circles), Northwest Lau Spreading Center (NWLSC; diamonds), Peggy Ridge/Lau Extensional Transform Zone (PR/LETZ; triangles), and the Central Lau Spreading Center (CLSC; squares). Degassing paths, shown by the dashed gray (closed system) and dashed black (open system) lines, are calculated using Volatile Calc [*Newman and Lowenstern*, 2002] with the following constraints: 49 wt.% SiO_2, 1.4 wt.% H_2O, 240 ppm CO_2, 1000°C, and for closed system degassing 0.5 wt.% exsolved volatiles. (b) Plot of hydrostatic pressure at collection depth versus pressure of volatile saturation (see Figure 2a) for glasses from the NW Lau basin. A 1:1 line is plotted with an uncertainty in collection pressure of 50 bars, to account for the possibility that lava flowed downhill from the initial eruption site.

of H_2O content, which we reference here to $H_2O_{(8.0)}$ (i.e., glass H_2O concentration corrected for fractional crystallization to the equivalent concentration at 8 wt. % MgO; Table S2 in Text S2), calculated using the expression of *Taylor and Martinez* [2003]. Figure 3a shows the functional form of the expression for $H_2O_{(8.0)}$, and the discriminating curve between glasses with low H_2O (<0.3 wt.% $H_2O_{(8.0)}$) and those with high H_2O (>0.3 wt.% $H_2O_{(8.0)}$). The contrast in LLDs of end-member parent magmas for H_2O-rich and H_2O-poor groups show the effects of H_2O on plagioclase and clinopyroxene suppression in hydrous magmas during crystallization. Figures 3b–3d show variations in Al_2O_3, CaO, and CaO/Al_2O_3 ratio as MgO decreases, which track the appearances of plagioclase and clinopyroxene on the liquidus during crystallization. The wetter magmas are consistent with later saturation of both plagioclase and clinopyroxene, an observation that is matched well by fractional crystallization models generated using Petrolog3 software for two parental magmas with different H_2O contents [*Danyushevsky and Plechov*, 2011] (see Figure 3 caption for details). These modeled shifts in saturation of plagioclase (plag) and clinopyroxene (cpx) due to melt H_2O content can be referenced to the MgO content of the model melts at the point of mineral saturation. For the drier melts, MgO content at plag-in (i.e., $MgO_{plag\text{-}in}$) is 9.2 wt.% and $MgO_{cpx\text{-}in}$ is at 8.6 wt.%, whereas for the wetter melts, $MgO_{plag\text{-}in}$ = 8.9 wt.% and $MgO_{cpx\text{-}in}$ = 7.1 wt.%.

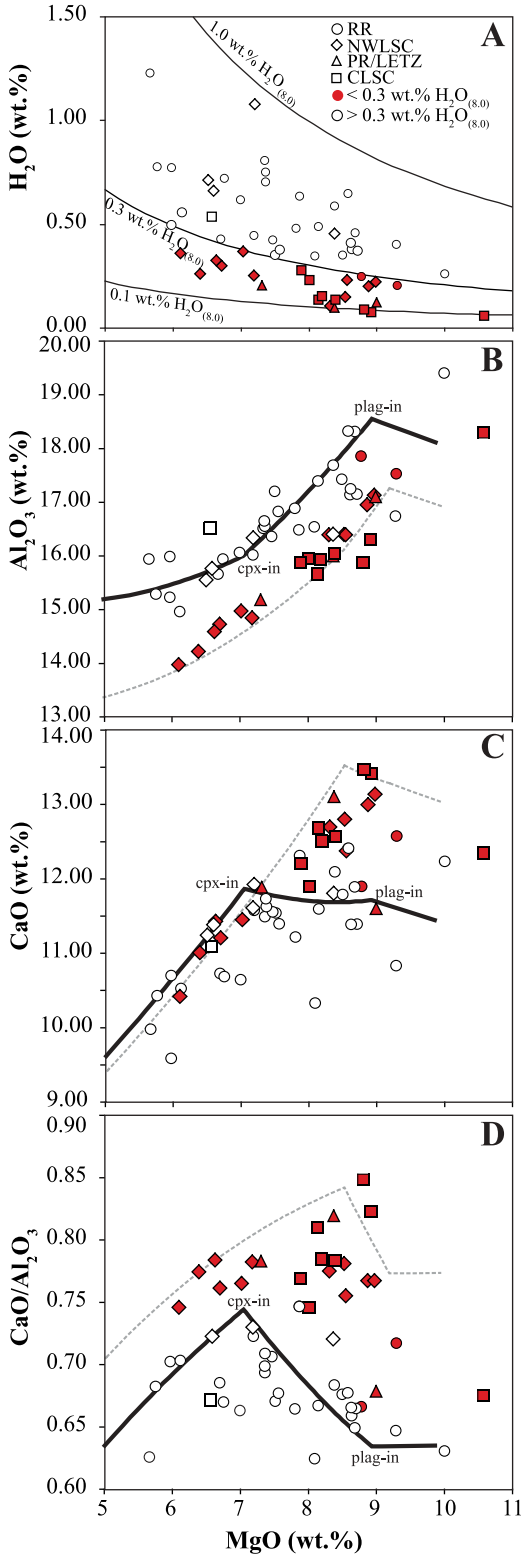

Figure 3. Plots of MgO versus major elements and ratios in glasses from the NW Lau basin, showing samples from Rochambeau Rifts (RR; circles), Northwest Lau Spreading Center (NWLSC; diamonds), Peggy Ridge/Lau Extensional Transform Zone (PR/LETZ; triangles), and the Central Lau Spreading Center (CLSC; squares). Shaded symbols contain <0.3 wt.% $H_2O_{8.0}$ and open symbols contain >0.3 wt.% $H_2O_{8.0}$. Liquid lines of descent are shown on Figures 3b–3d, modeled using Petrolog3 [*Danyushevsky and Plechov*, 2011] for two compositionally different theoretical parental melts with different primary H_2O contents (Table S3 in Text S2). The black solid line is for the wet parent magma and the gray dashed line is for the dry parent magma (Figures 3b–3d). (a) Plot of MgO versus H_2O. Thin lines show predicted variations of H_2O during fractional crystallization for variable initial H_2O contents, used to constrain $H_2O_{8.0}$ [*Taylor and Martinez*, 2003]. NW Lau samples are divided into two categories, those with <0.3 wt.% $H_2O_{8.0}$ (shaded symbols) and those with >0.3 wt.% $H_2O_{8.0}$ (open symbols). (b) Plot of MgO versus Al_2O_3. Points of plag-in and cpx-in are identified on the solid black line. (c) Plot of MgO versus CaO. (d) Plot of MgO versus CaO/Al_2O_3.

[12] The differences in major element composition of the two end-member parental magmas likely reflect differences in melting processes and/or source composition. Specifically, the wetter parent magma has higher Na_2O and Al_2O_3, lower CaO,

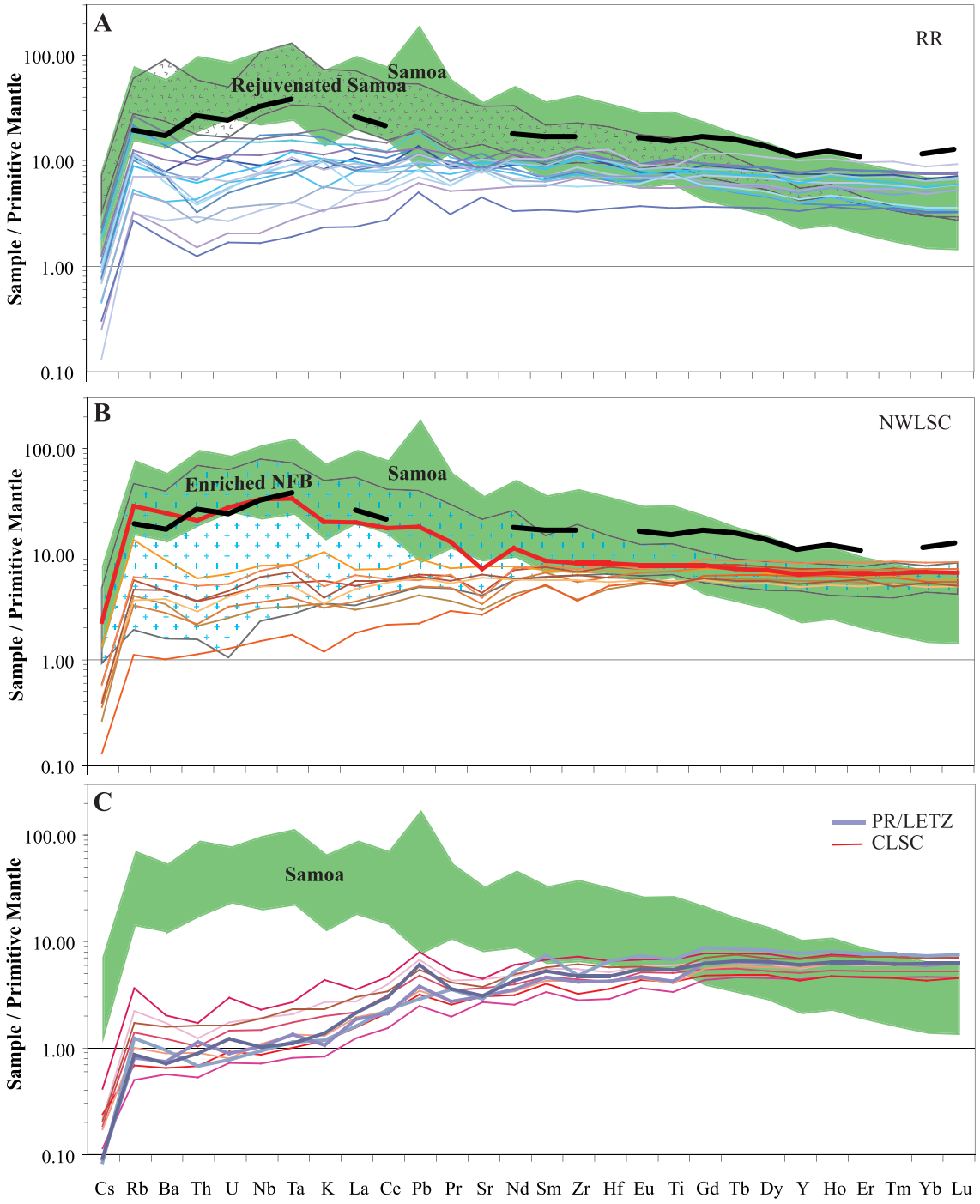

Figure 4. Primitive mantle-normalized trace element diagrams for glasses from the NW Lau basin. The field for the Vai trend of Samoan shield-stage volcanics [*Workman et al.*, 2004, 2006; *Jackson et al.*, 2007b, 2010] is shown by the solid shaded region for reference. (a) Select Rochambeau Rifts glasses are shown by the blue lines, and a field for the rejuvenated-stage Samoan lavas [*Jackson et al.*, 2010] is textured with carat symbols. The heavy black line shows the composition of a 6% fractional melt of the Ta'u Samoan mantle source of *Jackson et al.* [2007a] using bulk D's from *Kelley et al.* [2006]. This composition also is shown by the 6% tick mark along the dashed gray line in Figure 8b that tracks variable degree melts of the Ta'u source. (b) Select NWLSC glasses are shown by the orange lines. The most Nb-enriched NWLSC glass (samples NLD-44-01, NLD-44-02) is highlighted as a heavy line. Lavas from the N160 segment of the North Fiji Basin are encompassed by the field textured with crosses. The heavy black line is the same 6% fractional melt of the Ta'u as in Figure 4a. (c) Select glasses from PR/LETZ (gray-purple lines) and glasses from CLSC (red lines).

and a lower CaO/Al_2O_3 ratio than the dry parent magma. Higher concentrations of incompatible elements (e.g., Na_2O, Al_2O_3, H_2O) could reflect lower extents of melting of more hydrous mantle [e.g., *Langmuir et al.*, 1992; *Asimow and Langmuir*, 2003], although all incompatible elements should be affected similarly if this were the case, and no difference is required in TiO_2, K_2O, or P_2O_5 for the parental magmas. The difference may instead reflect variation in the modal cpx content of the mantle source, which will tend to drive melt compositions to higher Na_2O and Al_2O_3, and lower CaO/Al_2O_3 ratio with increasing source fertility (i.e., higher modal cpx [*Klein and Langmuir*, 1987]). It is important to note, however, that the parent magmas were chosen to bracket the majority of the data, which represent more of a compositional continuum rather than two discrete populations of melts.

3.3. Trace Element Variability

[13] The NW Lau Basin basalts span a wide range of trace element enrichment, as shown on Figure 4. The RR basalts (Figure 4a) range from highly depleted to highly enriched, but none fall completely within the fields defined by either Samoan shield-stage or rejuvenated magmatism. At the NWLSC, basalts are less enriched overall compared to RR (Figure 4b), although two samples (NLD-44-01, NLD-44-02) have distinct trace element patterns and are significantly more enriched than other samples from NWLSC or RR. These samples nearly overlap the Samoan field, although they have flat rather than sloping heavy rare earth elements, and are also encompassed by the field for basalts from the neighboring North Fiji Basin (NFB), which lies to the west of the study area (Figure 1). Trace element patterns for PR/LETZ and CLSC basalts show that these are less enriched than either RR or NWLSC, and are likely to be representative of the background depleted MOR-type mantle beneath the Lau Basin.

3.4. Isotope Variability

[14] The Sr and Nd isotopes of two RR samples, NLD-07-01 and NLD-20-01, overlap the least radiogenic part of the Samoan field (Figure 5c). *Tian et al.* [2011] report Sr-Nd isotopes for two other similar samples from RB. These are the only basalts in the NW Lau Basin with radiogenic enough Sr to match Samoan basalts. Our samples, especially NLD-20-01, also overlap the Samoan field in Hf-Nd and Pb isotope space (Figure 5d and auxiliary material). The Sr, Nd, Hf, and Pb isotopes of all other samples from both the RR and NWLSC are much more depleted than Samoa, with MORB-like ratios similar to the CLSC, although $^3He/^4He$ ratios in all of these samples range from 12 to 28 and show no correlation with any of the radiogenic isotopes (Figures S5d–S5e).

4. Discussion

[15] Trace element abundances and $^3He/^4He$ ratios show that the mantle beneath the NW Lau Basin is geochemically enriched relative to normal MORB or the proximal CLSC. Here, we explore the geospatial patterns of mantle enrichment, and the relationships between $^3He/^4He$ and these new data, in order to assess the identities and locations of distinct mantle components contributing to magmatism in the NW Lau Basin. In addition, we model the pressure and temperature conditions of mantle melting beneath NW Lau in order to test for a regional thermal gradation possibly associated with the Samoan Plume.

4.1. The Spatial Distribution of Enrichment in NW Lau

[16] The NW Lau samples span a wide range of enrichment, as shown on Figure 4, with a general trend of enrichment in incompatible trace elements broadly decreasing from the north (RR) to the south (CLSC). If Samoan material were simply migrating into the Lau Basin, the expectation would be that "Samoa-like" affinity or enrichment should decrease with latitude toward the south. Looking at the main tracer for Samoan affinity, the $^3He/^4He$ ratio, *Lupton et al.* [2009] compared $^3He/^4He$ ratios to latitude, showing a broad distribution of elevated $^3He/^4He$ ratios in the north and MORB-like ratios in the south (Figure 6c). Because Samoan lavas are enriched in light rare earth elements (LREE) and large ion lithophile elements (LILE), these indices of mantle enrichment (e.g., La/Sm, Ba/La) should also show a similar distribution of enrichment from north to south.

[17] Indices of enrichment do broadly decrease toward the south, as does the $^3He/^4He$ ratio (Figure 6), but neither a simple, secular change in these ratios with latitude exists, nor is the contrast purely bimodal (i.e., enriched in the north, depleted in the south). For example, Figure 6a shows two samples from NWLSC that are more enriched than any samples from RR to the north, whereas the Ba/La ratios in Figure 6b span the same range of values (5–15) for both RR and NWLSC. The RR and

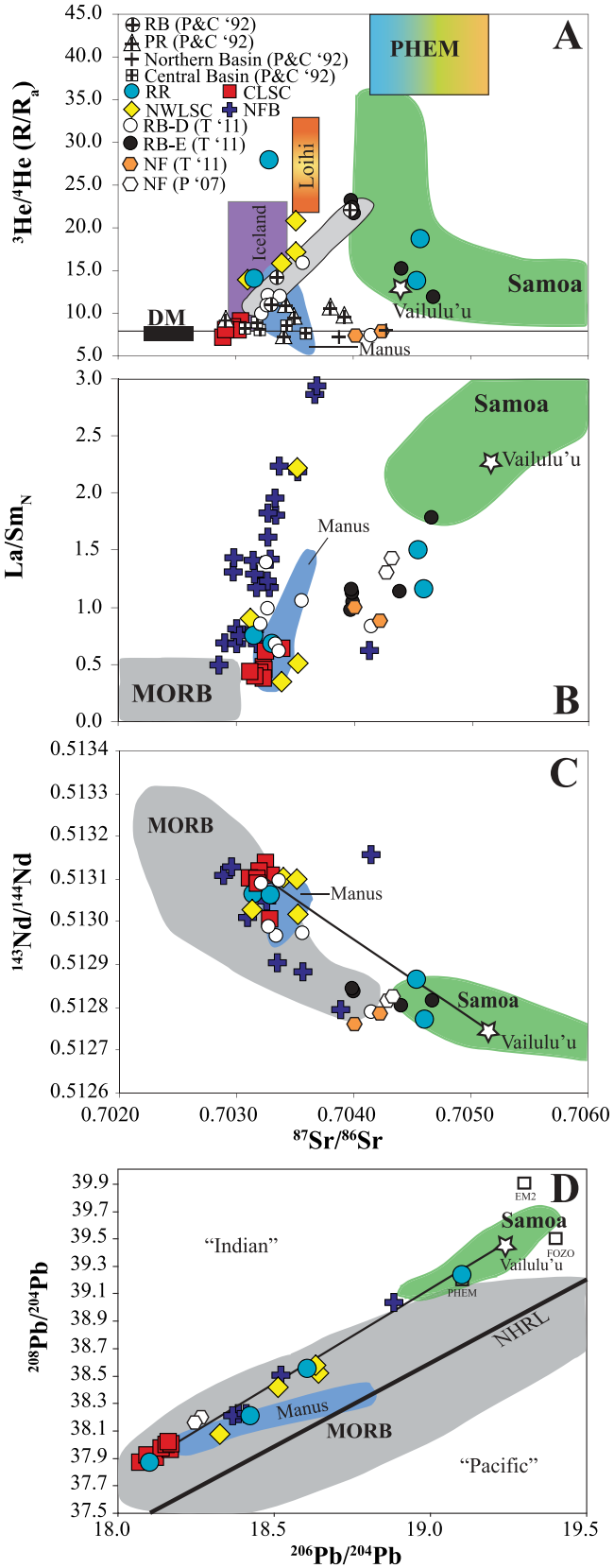
A
RB (P&C '92)
PR (P&C '92)
Northern Basin (P&C '92)
Central Basin (P&C '92)
RR
CLSC
NWLSC
NFB
RB-D (T '11)
RB-E (T '11)
NF (T '11)
NF (P '07)
PHEM
Loihi
Iceland
Samoa
Vailulu'u
DM
Manus
$^3He/^4He\ (R/R_a)$
B
Samoa
Vailulu'u
Manus
MORB
La/Sm_N
C
MORB
Manus
Samoa
Vailulu'u
$^{143}Nd/^{144}Nd$
$^{87}Sr/^{86}Sr$
D
EM2
Samoa
FOZO
Vailulu'u
PHEM
"Indian"
NHRL
Manus
MORB
"Pacific"
$^{208}Pb/^{204}Pb$
$^{206}Pb/^{204}Pb$

Figure 5

NWLSC span large ranges, from highly enriched to highly depleted, with no apparent geographic trends, and the PR and CLSC are uniformly similar to MORB. Furthermore, the trace elements do not clearly correlate with $^{3}He/^{4}He$ (Figure 6d), as would be expected if the source of enrichment were a single mantle component.

4.2. Constraining the Influence of Subduction on NW Lau Mantle Sources

[18] One source of enrichment that could perturb correlations of trace elements with He isotopes is subduction, which is not known to significantly modify $^{3}He/^{4}He$ ratios of magmas [*Poreda and Craig*, 1989], but can enrich light REE and Ba/La ratios by way of fluid and sediment melt additions to the mantle source. Although the NW Lau Basin is located ~530 km from the active Tonga subduction zone, the basin is opening in a region of paleo-subduction and the possibility for lingering influence from the past subduction along the Vitiaz Lineament remains. We test for effects of subduction on the mantle source beneath NW Lau by examining classic fluid- and sediment melt-mobile elements (i.e., Ba, Pb, H_2O, LREE).

[19] Extensive study of the ELSC provides a framework for comparing the NW Lau lavas with other regional lavas with well-established subduction influence [e.g., *Bézos et al.*, 2009; *Escrig et al.*, 2009]. Figure 7a compares two important ratios that are sensitive to subduction influence, Ba/La and H_2O/Ce. As slab-derived fluids rich in H_2O and Ba are added to the mantle, both of these ratios will increase, as both La and Ce partition less strongly than Ba into aqueous fluid released from the subducting slab. Although the lavas from RR and NWLSC extend to higher Ba/La ratios than Samoa, they show no coincident increase in H_2O/Ce such as the trend shown by the ELSC.

[20] Other ratios sensitive to subduction influence are Nb/Nb* and the Ce/Pb ratio, shown in Figure 7b. Negative Nb anomalies (Nb/Nb* < 1, where Nb* is the projected concentration of Nb based on neighboring Th and La abundances) are characteristic of subduction-influenced magmas and correlate, as defined here, with increasing Th and La additions relative to comparatively immobile Nb from the slab to the mantle source. The Ce/Pb ratio also decreases as fluids are added from the slab to the mantle source, as both elements behave similarly during mantle melting (normal MORB Ce/Pb = 15–28), but fluid-mobile Pb is preferentially transported by the slab-derived mass flux resulting in lower Ce/Pb for arc magmas [*Miller et al.*, 1994]. The NW Lau basalts from RR and NWLSC have no significant negative Nb anomalies (Nb/Nb* ≥ 1) and Ce/Pb ratios ≥15, consistent with the range for normal MORB [*Miller et al.*, 1994] and inconsistent with the trend among subduction-influenced basalts from the ELSC, which have both Nb/Nb* ≤ 1 and Ce/Pb in most samples <15 (Figure 7b). Based on these observations, we find no evidence for subduction influence on the composition of the mantle beneath the NW Lau Basin.

4.3. Geochemical Characteristics of NW Lau Mantle Sources

[21] Since we have ruled out subduction as a possible process for adding contaminants to the mantle source, and Figure 6d rules out simple two-

Figure 5. Radiogenic isotopes and trace element plots for NW Lau Basin samples. (a) $^{87}Sr/^{86}Sr$ versus $^{3}He/^{4}He$, showing samples from RR (circles), NWLSC (diamonds), PR/LETZ (triangles), and CLSC (squares). The $^{3}He/^{4}He$ data for the samples from this study is from *Lupton et al.* [2009]. The shaded samples are from this study, the open and black circles, open triangles, and shaded hexagons are from *Tian et al.* [2011] and *Hahm et al.* [2012], the crossed symbols are from *Poreda and Craig* [1992], and the filled crosses are from the North Fiji Basin and open hexagons are from Niuafo'ou [*Pearce et al.*, 2007]. The field for the Vai trend of Samoan shield-stage volcanics [*Workman et al.*, 2004, 2006; *Jackson et al.*, 2007b, 2010] is shown by the solid shaded region for reference. An average composition for Vailulu'u is indicated by the white star within the Samoan field. Shaded fields for Manus Basin [*Shaw et al.*, 2004, 2012; *Sinton et al.*, 2003], Iceland [*Condomines et al.*, 1983; *Poreda et al.*, 1992], Loihi [*Craig and Lupton*, 1976; *Rison and Craig*, 1983; *Kurz et al.*, 1983], depleted mantle [*Poreda and Craig*, 1992], and Primitive Helium Mantle (PHEM) [*Farley et al.*, 1992] are shown for reference. The thin line is the average MORB $^{3}He/^{4}He$ ratio of 8. (b) Plot of $^{87}Sr/^{86}Sr$ versus La/Sm_N. The field for MORB (Table S5 in Text S2; compiled from PetDB; http://www.petdb.org), is shown by the solid gray shaded region for reference. (c) Plot of $^{87}Sr/^{86}Sr$ versus $^{143}Nd/^{144}Nd$. The solid black line shows mixing between a depleted CLSC-like end-member and an enriched Samoan-like end-member (e.g., Vailulu'u). (d) Plot of $^{206}Pb/^{204}Pb$ versus $^{208}Pb/^{204}Pb$. The solid black line shows mixing between a depleted CLSC-like end-member and an enriched Samoan-like end-member (e.g., Vailulu'u). The thick solid black line is the Northern Hemisphere Reference Line [*Hart*, 1984]. Black squares represent the fields for the enriched mantle end-member EMII [e.g., *Workman et al.*, 2004], primitive helium mantle (PHEM) [*Farley et al.*, 1992], and global hot spot mantle component ("FOZO" [*Hart et al.*, 1992]).

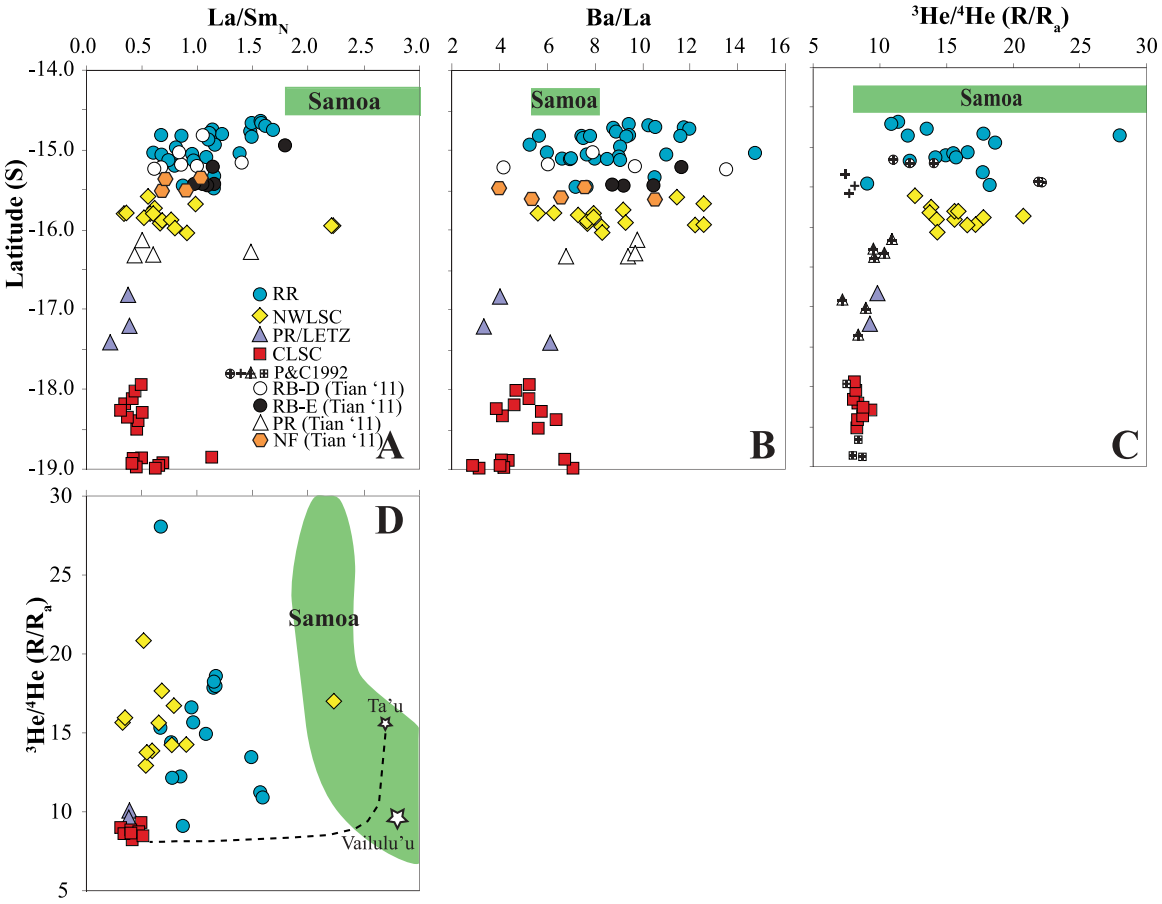

Figure 6. Trace element characteristics of NW Lau basin glasses as function of spatial distribution and He isotopic composition. Symbol notation is the same as in Figure 5. The dashed mixing line is between an average CLSC source and Ta'u source [*Jackson et al.*, 2007a]. (a) Plot of La/Sm$_N$ (chondrite normalized) versus latitude (°S). (b) Plot of Ba/La versus latitude (°S). (c) Plot of ^{3}He/^{4}He versus latitude (°S). (d) Plot of La/Sm$_N$ versus ^{3}He/^{4}He (R/R$_A$; R = ^{3}He/^{4}He and R$_a$ = R$_{air}$ = 1.39 * 10^{-6}).

component mantle mixing, more complex processes may be required to explain the variations seen in the NW Lau basalts. Here, we explore the trace element and isotopic signatures of the NW Lau basalts, and attempt to identify the number of possible mantle sources beneath NW Lau and their geochemical characteristics.

[22] Although developed for exploring mixing between Th and LREE-enriched subducted sediment and LREE-depleted mantle components beneath arc volcanoes [*Plank*, 2005], Figure 8a can also be more generally applied to explore mixing between any two relatively enriched and depleted mantle components. In the case of NW Lau, possible mantle sources include MORB mantle (low Th/La, high Sm/La) and an enriched source like Samoa (high Th/La, low Sm/La). The NW Lau basalts fall on straight-line mixing trajectories between an enriched mantle that lies within the Samoan field and two distinct components of background depleted mantle that are spanned by the data array for the CLSC. The Sm/La ratio can, however, be fractionated by melting a common mantle source to variable extents, so the variation in the MORB component from RR and NWLSC may be inherent variation in the MORB mantle source beneath NWLSC. In contrast, Figure 8b suggests possible variation in the enriched component, as traced by Rb/Zr and Nb/Zr ratios. The field for Samoa is constrained by Nb/Zr = 0.12–0.25 and Rb/Zr > 0.05, whereas normal MORBs have very low Nb/Zr and Rb/Zr ratios. The most enriched samples from RR point toward mixing with a Rb and Nb-enriched component that may be similar to Samoa. Two samples from dredge 44 on the NWLSC, are most extreme, fall outside the field for Samoa, and are similar to some samples from the neighboring NFB. In addition, samples from Rochambeau Rifts define a separate trend

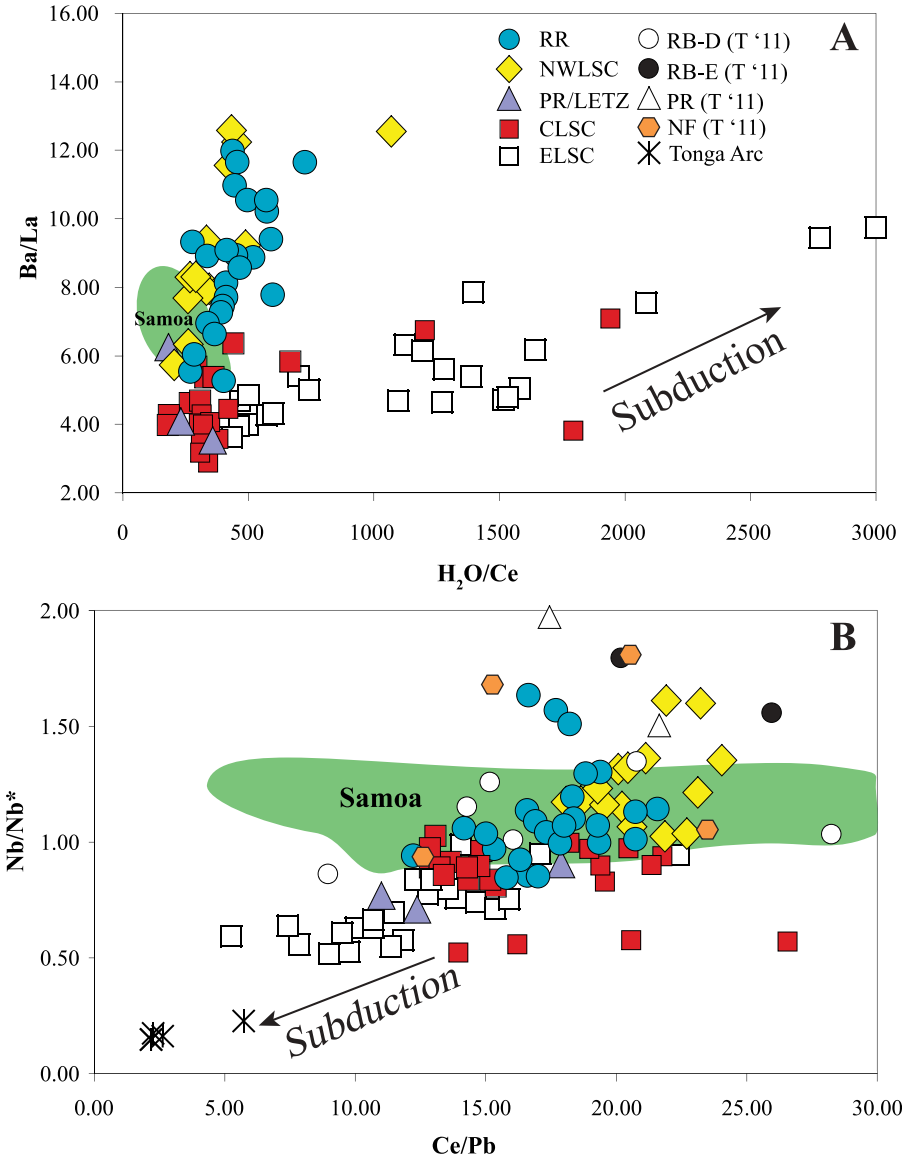

Figure 7. (a) Plot of H_2O/Ce versus Ba/La, showing samples from RR (circles), NWLSC (diamonds), PR/LETZ (triangles), and CLSC (squares). Symbol notation is the same as in previous figures. The open squares are ELSC samples from *Bézos et al.* [2009], and the asterisks are Tonga Arc glasses from *Cooper et al.* [2010]. The field for MORB, encompassing East Pacific Rise MORB glasses (Table S8 in Text S2; compiled from PetDB; http://www.petdb.org), is shown by the solid gray shaded region for reference. The arrow illustrates the trend of subduction influence, shown by select CLSC and ELSC samples, of increasing Ba/La with increasing H_2O/Ce. (b) Plot of Ce/Pb versus Nb/Nb*. Nb* is the projected concentration of Nb based on Th and La abundances, where Nb/Nb* is calculated as $Nb_N/(Th_N \times La_N)^{1/2}$. The arrow illustrates the trend of subduction influence, shown by select CLSC, ELSC, and Tonga Arc samples, of decreasing Nb/Nb* with decreasing Ce/Pb.

from NWLSC in Figure 8b as well as Figure 8a, indicating a different enriched component, and the samples that are most similar isotopically to the Vai Trend in Samoa lie on this trend. Initial interpretations drawn from Figure 8 thus suggest that there are a minimum of two, but possibly up to four mantle components involved in magma production beneath NW Lau, with trace element characteristics similar to regional basalts erupted at the CLSC (both enriched and depleted), Samoa, and NFB.

[23] The number of possible mantle components may be further refined using He, Sr, Nd, Pb, and Hf isotopes, which are particularly important geochemical tracers of mantle sources, as isotopes are insensitive to fractionation by melting and crystallization processes.

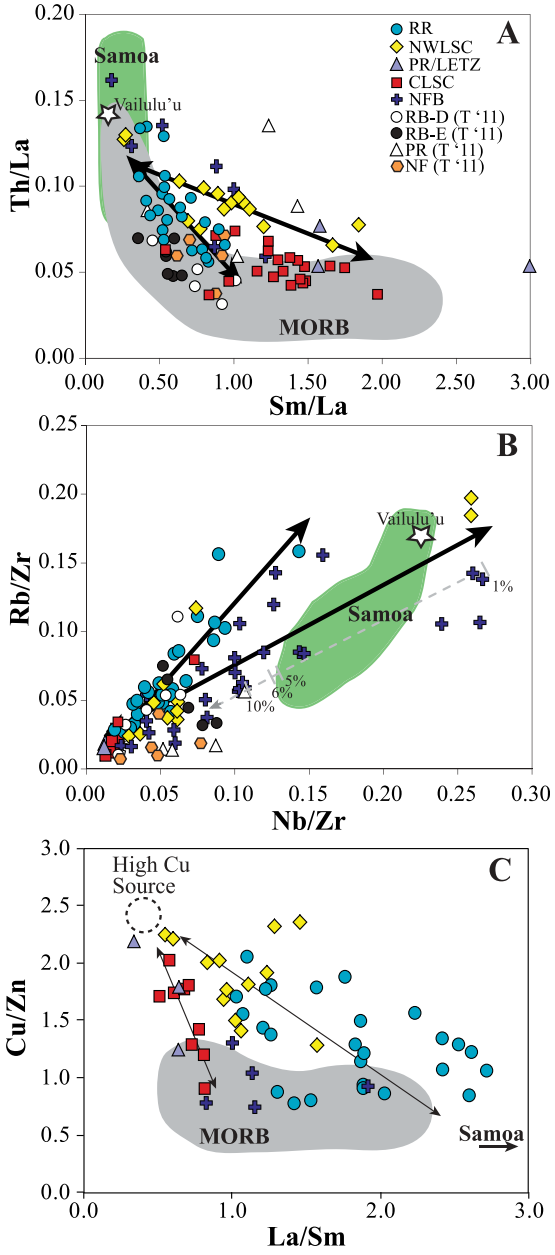

Figure 8. (a) Plot of Sm/La versus Th/La, showing samples from RR (circles), NWLSC (diamonds), PR/LETZ (triangles), and CLSC (squares). Symbol notation is the same as in previous figures. The black lines indicate mixing trends between an enriched, possibly Samoa-like source and two different depleted MORB-like end-members. (b) Plot of Nb/Zr versus Rb/Zr. The gray dashed line is a fractional melting model tracking variable degree melts of the Ta'u source (*Jackson et al.* [2007a]; bulk D's from *Kelley et al.* [2006]; see Figure 4 caption for details). (c) Plot La/Sm versus Cu/Zn for NW Lau basalts >6.0 wt.% MgO. The small symbols for MORB are from *Jenner and O'Neill* [2012].

Figure 5a (data from *Poreda and Craig* [1992]) shows the relationships between $^{3}He/^{4}He$ and $^{87}Sr/^{86}Sr$ in regional lavas from Samoa, RB, and our new samples from NW Lau. The low $^{3}He/^{4}He$, high $^{87}Sr/^{86}Sr$ component of Samoa is considered an end-member mantle composition termed EMII [e.g., *Workman et al.*, 2004]. The high $^{3}He/^{4}He$, low $^{87}Sr/^{86}Sr$ component of Samoa was initially dubbed "primitive helium mantle" (PHEM) [*Farley et al.*, 1992], although other work has shown that a similar mantle component may be common to most global hot spots ("FOZO" [*Hart et al.*, 1992]). Depleted MORB mantle (DMM) is characterized by both low $^{3}He/^{4}He$ (7–9 R_a) and low $^{87}Sr/^{86}Sr$ ratios (0.7022–0.7026). Four samples from the RB region [*Poreda and Craig*, 1992] originally suggested a straight-line trend between DMM and Samoa (Figure 5a). *Tian et al.* [2011] found that samples from RB consist of two groups, one that is depleted with a MORB-like, minor subduction signature and one that is enriched by a Samoa-like shield magmatism signature. Our new data show that two samples from RR do plot with Samoa in He, Sr, and Nd isotopes, although six others from RR and NWLSC do not (including the highest $^{3}He/^{4}He$ sample at 28 R_a). On Figure 8a, these six samples instead point to greater enrichment in $^{3}He/^{4}He$ at a given $^{87}Sr/^{86}Sr$, which are characteristics more typical of other hot spots like Iceland or Loihi, suggesting an alternate mantle source for some of the high $^{3}He/^{4}He$ beneath NW Lau.

[24] Strontium isotopes coupled with trace element ratios and Nd isotopes tell a similar story. Figures 5b and 5c show the La/Sm and $^{143}Nd/^{144}Nd$ ratios versus $^{87}Sr/^{86}Sr$, and the NW Lau data show two fairly distinct behaviors. The RR samples with the highest $^{87}Sr/^{86}Sr$ point toward a Samoa-like composition. These, coupled with two RB samples from *Tian et al.* [2011], are the only basalts from anywhere in the northern Lau Basin that have clear Samoan isotopic traits. The remaining samples from both the NWLSC and RR cluster with MORB-like LREE, $^{143}Nd/^{144}Nd$, and $^{87}Sr/^{86}Sr$, with the exception of the strongly trace element enriched sample from NWLSC, which is isotopically similar to the other samples, but similar in LREE to lavas erupted in the NFB. Taken alone, the isotopic data from our study require at least two mantle components beneath NW Lau, but do not clearly resolve any other isotopically distinct source. *Tian et al.* [2011] found isotopic variations at RB that appear to require a third mantle component of sorts, with lower $^{87}Sr/^{86}Sr$ at a given $^{143}Nd/^{144}Nd$, that they linked to the "rejuvenated" component of Samoan

magmatism (Figure 5c). Lead isotopes (Figure 5d) also suggest mixing between a minimum of two mantle sources beneath NW Lau. One component is an Indian-type MORB mantle, the other is strongly enriched in Pb isotopes in the direction of Samoan basalts, with one RR sample falling within the Samoan field. If a third source, similar in composition to that beneath the NFB, were involved beneath NW Lau, it would not be clearly discriminated by Pb isotopes because enriched NFB basalts overlap with Samoa in Pb isotopic composition (Figure 5d).

4.4. Modeling Mantle Melting Conditions Beneath the NW Lau Basin

[25] Hot spots such as Samoa are characterized by elevated mantle potential temperature, [e.g., *Putirka*, 2008] resulting in higher extents of melting of an adiabatically upwelling mantle. Subduction influence within the mantle source of NW Lau appears largely absent, thus magma production in this region should therefore be a simple function of mantle potential temperature coupled with the inherent composition of the mantle source. Melting beneath mid-ocean spreading ridges is driven by adiabatic upwelling of the mantle over a range of mantle potential temperatures [*Klein and Langmuir*, 1987, 1989]. If a hot plume were infiltrating the Lau Basin, however, we may also expect elevated mantle temperature in the region, possibly cooling off with distance from the plate boundary. Recent estimates of the Samoan mantle potential temperature place it at ~1720°C [*Putirka et al.*, 2007], whereas previous constraints from the Northern Lau Basin indicated a regional mantle potential temperature of ~1460°C [*Falloon et al.*, 1999] to ~1400°C [*Kelley et al.*, 2006]. The seismic structure beneath the CLSC shows low velocity zones (V_p and V_p/V_s), interpreted as melt regions, located 30–50 km beneath the CLSC, consistent with a regional T_p of ~1400°C [*Conder and Wiens*, 2006].

[26] Accurate petrological constraints on mantle temperatures and melting conditions require that basalt compositions be corrected for the effects of fractional crystallization and referenced to a common point along the liquid line of descent (LLD). The LLD modeling done here (see Text S1, section S.5) allows reconstruction of melts to their primary compositions by using the modeled fractionation slopes to project melt compositions back to the points of cpx-in and plag-in (Table S6 in Text S2 and Figure S4) before adding equilibrium olivine to each melt until it is in equilibrium with Fo_{90} (Table S7 in Text S2). A detailed summary of the correction procedure is provided in the auxiliary material. The pressures and temperatures of last equilibration of each reconstructed primary melt with the mantle are calculated using a thermobarometer based on the Si, Mg, and Fe contents of primary melts in equilibrium with olivine + orthopyroxene [*Lee et al.*, 2009]. The model requires an estimate of the iron oxidation state [i.e., $Fe^{3+}/(Fe^{3+} + Fe^{2+})$] in the magma, which here is taken as a normal MORB value (0.16 [*Cottrell and Kelley*, 2011]).

[27] The results of this modeling show that melt equilibration pressure increases toward the plate boundary in the north (RR 1.38 GPa; CLSC 1.08 GPa; Figure 9a). The higher pressures of equilibration could be the result of a hotter mantle intersecting the solidus at greater depth beneath RR and NWLSC. The modeled equilibration temperatures, however, show that the higher pressure melts at RR are cooler, not hotter, than basalts from NWLSC or CLSC (Figure 9c, inset), suggesting that temperature may not exert the main control over the melting pressure. Alternatively, mantle composition variations in the north may be responsible for melting at a deeper mantle solidus.

[28] Among a number of compositional factors known to lower the peridotite solidus is the H_2O content [e.g., *Kushiro*, 1968]. We calculated the water content of the NW Lau mantle sources using the batch melting model and Ti/Y source composition model from *Kelley et al.* [2006], using $TiO_{2(Fo90)}$ concentration as a proxy for melt fraction (see auxiliary material). The water content of the mantle source (i.e., $C^0_{H_2O}$) beneath NW Lau increases northward, toward the plate boundary, in a manner similar to the melt equilibration pressure (Figure 9b). Higher $C^0_{H_2O}$ lowers the mantle solidus temperature, allowing hydrous melting to take place at lower temperatures and higher pressures relative to dry peridotite, shown on Figure 9c, modeled using the parameterization of *Kelley et al.* [2010]. Adiabatic melting paths (see Figure 9 caption for details) for mantle of a constant potential temperature (T_p = 1400°C) are shown on Figure 9c intersecting dry and hydrous peridotite solidi for a range of $C^0_{H_2O}$ relevant to the Lau samples. Melting of a mantle with homogeneous T_p but heterogeneous H_2O content may explain the spread in the modeled P-T conditions, and explain the higher average pressures of melt equilibration in the northern part of the basin.

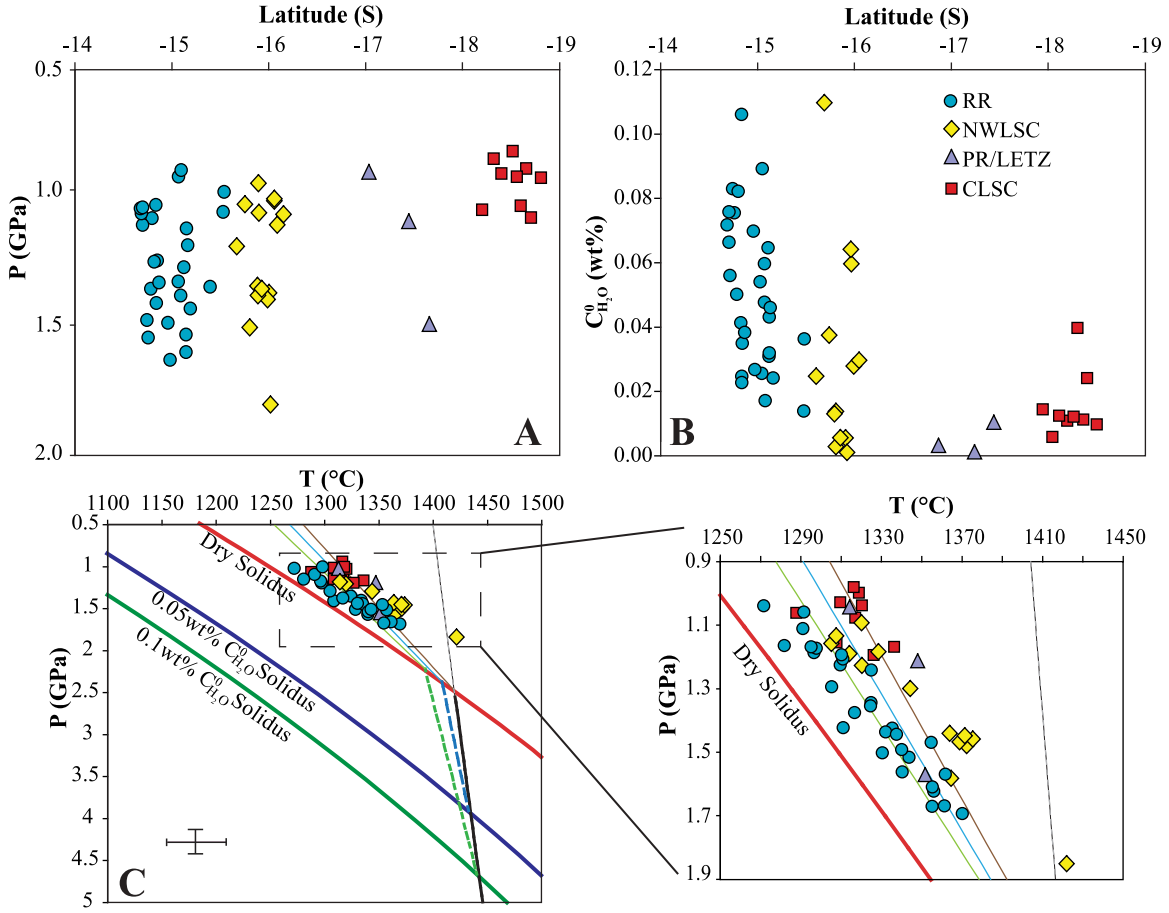

Figure 9. (a) Plot of latitude (°S) versus pressure for NW Lau basalts, showing samples RR (circles), NWLSC (diamonds), PR/LETZ (triangles), and CLSC (squares). (b) Plot of latitude (°S) versus $C^0_{H_2O}$ for NW Lau basalts. (c) Plot of temperature versus pressure for NW Lau basalts, showing the same symbols as Figure 9a. The dry solidus is from *Hirschmann* [2000], the two wet solidi are for $C^0_{H_2O}$ of 0.05 wt.% and 0.1 wt.% [*Kelley et al.*, 2010]. The solid black line is the adiabat for a mantle potential temperature of ~1400°C. The two dashed lines are melt paths (slope = 2°C/kbar) for the two wet solidi, generated as the adiabat crosses each solidi [*Asimow et al.*, 2004], generating low amounts of F due to melting and the continuing dehydration of the surrounding mantle which reduces water-influenced melt productivity. The three thin lines are melt paths (slope = 7°C/kbar) above the dry solidus, a more productive melt regime, and the thin dashed line is the projected path of the adiabat [*Asimow and Langmuir*, 2003]. The outlined region shows the inset of the pressure-temperature diagram. Error bars are error associated with using the thermobarometer [*Lee et al.*, 2009].

Additionally, RR have lower HREE relative to MgO and other trace elements, consistent with more residual garnet present and greater depth of melting as a result of a wetter source. A constant mantle T_p of 1400°C from the northern plate boundary to the CLSC seems inconsistent with the model of migration of a hot plume into the NW Lau Basin. *Kelley et al.* [2006] inferred a much cooler mantle (T_p ~ 1300°C) in the southern part of the Lau Basin, suggesting that the scale of thermal variation may be different from that of geochemical variation. It is also possible that hot Samoan mantle could be thermally equilibrated with its surroundings by the time it reaches the plate boundary [*Druken et al.*, 2009].

4.5. Hypotheses for Sources of Enrichment and Mantle Flow Beneath NW Lau

4.5.1. Mixing Between Two Mantle Source Components

[29] Samoan geochemical data shown on Figures 5–8 are restricted to the Vai trend (Tau and Ofu islands and Vailulu'u seamount [*Workman et al.*, 2004]), which encompasses the high $^3He/^4He$ (>15) and low $^{87}Sr/^{86}Sr$ component of Samoan lavas. This is the classically hypothesized component contributing elevated $^3He/^4He$ in the Lau basin. Our detailed sampling and analysis of regional volcanism in the

NW Lau Basin reveals the influence of a minimum of two mantle sources beneath the NW Lau Basin, as originally proposed by *Turner and Hawkesworth* [1998], to explain the majority of the trace element and isotopic data reported here. Lead, strontium, and neodymium isotopes (Figure 5d) require two end-members: a Samoa-like enriched mantle source and a depleted "Indian" MORB-like mantle source. The first mantle source is similar to Samoa with respect to both trace elements and radiogenic isotopes, with elevated $^{3}He/^{4}He$ and radiogenic isotopic compositions similar to the Vai trend in Samoa (e.g., Figures 5, 6, 8, and S5). The second mantle source is a depleted, CLSC-type MORB source, with LREE depletion and MORB-like radiogenic isotopes indicative of an origin in the Indian mantle domain (Figures 5, 6, and S5).

[30] Following the same approach for calculating $C^{0}_{H_2O}$ (see section 4.4 above and auxiliary material), we also calculate the source trace element compositions of the NW Lau lavas (Figure S6) to test whether two component mixing is evident in the source compositions for the NW Lau samples. The samples from NW Lau show evidence for binary mixing between an enriched source and DMM [*Workman and Hart*, 2005]. The modeled theoretical enriched source, determined from the most enriched RR samples, is enriched in certain trace elements relative to Ta'u source (e.g., Ba, Nb, La, Th) but has Samoan-like isotopes (Figure 5 and Figure S6). The enriched source infiltrating NW Lau thus may represent part of the Samoan Plume that is not observed in the Samoan islands, but rather part of the plume that has been deflected toward NW Lau from depth.

[31] Figure 10a illustrates this scenario of a two component mixture of mantle sources beneath the NW Lau basin, with an important caveat. A simple two-component model satisfies the majority of trace element and Sr-Nd-Pb-Hf isotopic data, but fails to explain the He isotopes. The two-component model therefore must include an "invisible" third component that transports He from Samoa independent of geochemical characteristics or elevated T_p of the Samoan Plume. The Samoan mantle is known to be heterogeneous [e.g., *Jackson et al.*, 2010], but this scenario requires NW Lau to be sampling an enriched Samoan source with two components, a known Samoan source in trace element and isotopic composition related to the Vai trend, and a separate Samoan helium component that causes elevated $^{3}He/^{4}He$ ratios in lavas that are distinctly non-Samoan (e.g., MORB-like) in trace element and isotopic composition.

4.5.2. A Third Mantle Component?

[32] Although the majority of our trace element and isotopic data suggest only two mantle sources, a distinct, third mantle source could be present, following several other lines of evidence. In particular, the highly enriched samples from NWLSC, the coupled He-Ne isotope systematics, the chalcophile element contents, and some radiogenic isotope data point to alternate sources of compositional diversity in the mantle beneath NW Lau. Here, we discuss the data and reasoning behind these additional constraints, and consider the implications for mantle source models in the NW Lau region.

[33] We first explore whether variable degrees of melting of a binary mantle source can explain the observations that suggest more than two mantle sources for our samples (i.e., the most Nb-enriched NWLSC samples, and the differences between RR and NWLSC trends in Figure 8). The gray dashed line in Figure 8b shows the trajectory of variable percent melting of the Ta'u Samoan source [*Jackson et al.*, 2007a] (see Figure 4 caption for details of the model). The model can explain our and *Tian et al.*'s [2011] most Nb-enriched samples from the NWLSC but cannot explain the steeper trend for RR which is more like Ta'u isotopically. Figure 4b shows that although a 6% melt of the Ta'u source can approximate the Rb to La portion of the spider diagram for our most enriched NWLSC samples (NLD-44-01 and NLD-44-02), it predicts much higher middle and heavy REE concentrations. The match is even worse for the samples that are most like Tau isotopically (NLD-07-01 and NLD-20-01) because they have the lowest HREE contents and steepest REE patterns (Figure 4a). We conclude, therefore, that just varying percent melting of two mantle sources cannot explain our observations, and at face value, these enriched melts appear to require melting of a mantle source with similar isotopic composition, but different trace element characteristics, relative to the Ta'u source. Such an alternate mantle source, however, is restricted to these two samples and thus is highly localized beneath the NWLSC, and could not be responsible for broad, regional source heterogeneity.

[34] We next summarize observations that suggest involvement of additional mantle sources. *Jenner et al.* [2012] observed unusual enrichment in Cu

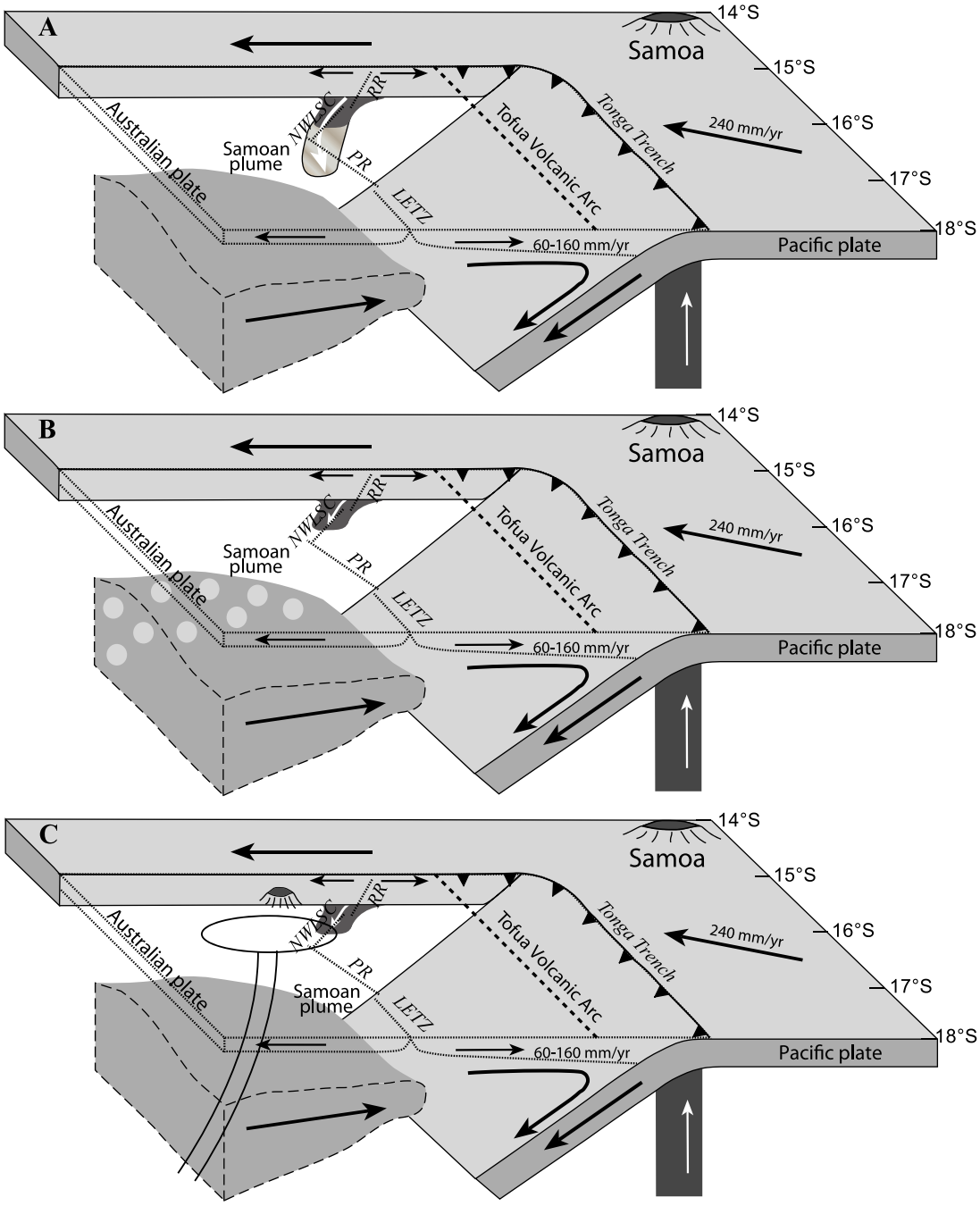

Figure 10. Three regional cartoons illustrating possible hypotheses for the origin of enriched mantle beneath the RR and NWLSC. (a) The first scenario invokes a contribution from an isotopically recognizable component of Samoan mantle and a separate, noble-gas-only component that causes enrichment in He isotopes without a proportional contribution from Samoan trace elements. (b) The second scenario invokes inherent mantle heterogeneity in the NW Lau mantle, unrelated to (or linked to, as in the case of RB) Samoa. (c) A third scenario, in which the N. Lau basin is infiltrated by a small quantity of Samoan mantle and is also impinged upon by a previously unidentified regional hot spot located to the west of the spreading centers and rift zone.

and Ag relative to MORB at the NWLSC, RR, and CLSC. They explained the data by mixing between a high Cu source and at least one low Cu source (Samoa and MORB are indistinguishable and low in Cu). The origin of the high Cu source was not identified, but we show on Figure 8c that enrichments in Cu over Zn correlate regionally with the La/Sm ratio. The most Cu-enriched samples from

both the CLSC and NWLSC have the lowest La/Sm ratios, suggesting that the high Cu source is the highly depleted MORB mantle that is most prominent beneath the NWLSC (Figure 8a). From this perspective, a third mantle source, dispersed throughout the NW Lau Basin, with depletions in lithophile trace elements and enrichments in chalcophile elements is needed to explain the data (e.g., Figure 10b).

[35] Although He does not correlate with trace elements and other isotopes, there is correlation between He and Ne. Recent studies by *Hahm et al.* [2012] and *Lupton et al.* [2012] found that He-Ne systematics identify the noble gas signature of the NW Lau lavas as a mixture of MORB and OIB, with characteristics similar to Samoan noble gases. Although *Hahm et al.* [2012] and *Lupton et al.* [2012] model the noble gas mixing using different OIB and MORB end-members, the mixing arrays from both studies suggest different contributions from, and possibly different compositions of, OIB and MORB sources among NW Lau samples (Figure S5). Samples from RB [*Hahm et al.*, 2012] plot with or below the trend defined by Samoa [*Jackson et al.*, 2009], whereas samples from RR and NWLSC [*Lupton et al.*, 2012] define an array above Samoa (Figure S5), effectively requiring different $^{3}He/^{22}Ne$ ratios in either the MORB or OIB end-members (or possibly both) beneath RB relative to the rest of the NW Lau Basin.

[36] *Tian et al.* [2011] explained the complex relationships among trace elements and radiogenic isotopes at the RB seamount by the impingement of Samoan Plume-related mantle upon the local subduction-metasomatized Indian-type mantle. They propose that two different Samoan components are required to explain the isotopic diversity of their data at RB. We find, however, that only two isotopically distinct components (one Samoan, and one MORB-like) are required to explain variations in our data set for these areas. If an additional enriched component, of the type identified by *Tian et al.* [2011], is present beneath the NW Lau Basin, our data indicate that it must be localized to the area beneath RB and is not widely dispersed through the regional mantle.

[37] We also note that the Manus Basin is another Pacific back-arc basin with elevated $^{3}He/^{4}He$ signatures, that is associated with locally elevated mantle temperature [e.g., *Kelley et al.*, 2006] and with a diffuse regional mantle plume [e.g., *Shaw et al.*, 2004; *Shaw et al.*, 2012]. The Manus Basin provides a regional example of elevated $^{3}He/^{4}He$ signatures without the presence of a clearly identified mantle plume, thus suggesting that the Samoan mantle is not the only possible source of high $^{3}He/^{4}He$ in the NW Lau Basin, and its proximity to the enrichments in NW Lau could simply be coincidence. In this view, the enriched component beneath the NW Lau Basin could be sourced by a diffuse local plume (e.g., Figure 10c), as has been suggested for the Manus Basin. Some basalts from the NW Lau Basin do, however, have trace element and isotopic characteristics in common with Samoan sources, making this hypothesis less likely.

[38] Models involving just two mantle sources cannot explain the lack of correlation between noble gases and other isotopes (Figure 5a), the details of trace element patterns (Figure 4b), and the differences in trace element trajectories between RR and NWLSC (Figures 8a and 8b). The consequences of these combined observations effectively suggest some alternate hypotheses to explain the diversity of trace elements, noble gases, and radiogenic isotopes. All hypotheses must include a known Samoan plume composition that is isotopically similar to Ta'u, and the alternate hypotheses presented here need not be mutually exclusive; indeed, a combination of these models may be required to explain all of the available data. The simplest model (Figure 10a) involves mixing of a MORB-like mantle with an enriched Samoan-like mantle composition, although a physically separate component carrying noble gases must move independently of the trace elements and isotopes from the Samoan Plume. In addition, to explain the enriched samples at NWLSC, as well as both the chalcophile element constraints [*Jenner et al.*, 2012] and the noble gas and radiogenic isotope constraints [*Tian et al.*, 2011; *Hahm et al.*, 2012; *Lupton et al.*, 2012] there may be inherent mantle heterogeneity beneath NW Lau Basin (Figure 10b). The Manus Basin model, where the basalts have a geochemical plume signature without an identified plume in the region [*Shaw et al.*, 2004, 2012], would permit a third hypothesis (Figure 10c), which invokes a previously unidentified regional hot spot with high $^{3}He/^{4}He$ located to the west of NW Lau Basin, to explain the similarities in trace element and isotopic signatures between some NW Lau basalts and NFB basalts.

4.5.3. Independent Behavior of Helium

[39] Although $^{3}He/^{4}He$ ratios do broadly correlate with trace elements and radiogenic isotopes at

Samoa (e.g., high $^3He/^4He$ ratios are restricted to a narrow range of $^{87}Sr/^{86}Sr$ ratios; Figure 5a), there is an obvious lack of correlation between $^3He/^4He$ and trace elements and radiogenic isotopes within the NW Lau Basin. The majority of samples from RR and NWLSC that have $^3He/^4He$ = 10–20 R_a are otherwise isotopically similar to MORB, whereas Samoan samples in the same range are isotopically enriched. Helium isotopes similar to Samoan ratios largely do not correlate with trace element or radiogenic isotopic enrichments characteristic of Samoan influence in the NW Lau Basin, although the combination of He and Ne isotopes fingerprint the noble gas signature as a mixture of MORB and OIB (similar to Samoa [*Hahm et al.*, 2012; *Lupton et al.*, 2012]). Processes such as degassing of the enriched melts [*Hahm et al.*, 2012] or diffusion of the noble gases (He and Ne [*Lux*, 1987]) could explain the lack of correlation between He and other radiogenic isotopes and trace elements. Helium and Ne degas faster than the other noble gases, which may result in an observed lack of correlations in enriched melts between He (and Ne) and other isotopes or noble gases [*Lux*, 1987; *Niedermann et al.*, 1997]. Another process that could result in He moving independently in the mantle is a "leaky lower mantle" scenario induced by rapid spreading rates [*Shen et al.*, 1995; *Niedermann et al.*, 1997]. This model was developed for fast spreading ridges (e.g., the East Pacific Rise), where fast spreading is associated with deep induced mantle flow that could pick up material introduced into the upper mantle by miniature plumes leaking upward from the lower mantle at the 670 km boundary. The NW Lau Basin is opening with extremely fast spreading rates (160 mm/yr in the north), and this process could thus also apply at NW Lau, causing elevated noble gas signatures, with normal MORB Sr-Nd-Pb isotopes. Another possibility is the Samoan Plume could be entering the NW Lau Basin in a chaotic manner due to the complex tectonics (e.g., fast subduction, tear in the subducting plate, and rapid upwelling of the mantle beneath the back-arc [*Hawkins*, 1995; *Millen and Hamburger*, 1998]. If the Samoan Plume is not entering the back-arc basin smoothly then a clean latitudinal decrease of the geochemical tracers might not be expected [*Spiegelman*, 1996].

5. Conclusions

[40] Our geochemical data for new samples from the NW Lau Basin suggest that two-component mixing of mantle sources is the simplest model required to explain magma generation beneath the NW Lau basin, although more complexity and several alternate sources may be permissible given the full range of available data. The simplest model involves mixing between a MORB-like mantle (e.g., CLSC) and an enriched mantle component with trace element and isotopic characteristics similar to Samoa, although this model requires He to migrate independently of trace elements from their Samoan source into the Lau mantle. Mantle potential temperature is relatively homogeneous throughout NW Lau, from RR to CLSC (~1400°C), although possibly hotter than the ELSC and Valu Fa ridges further south, but variations in primary melt equilibration pressure show increasing depth of equilibration toward the north (~1.08 GPa at CLSC; ~1.38 GPa at RR) that are explained by melting mantle of constant T_p but variable H_2O content. We present three alternative, though not mutually exclusive, hypotheses to explain the observed geochemical characteristics of NW Lau basalts, invoking both a contribution from an isotopically recognizable component of Samoan mantle and (1) a separate, noble-gas-only component that causes enrichment in He isotopes without a proportional contribution from Samoan trace elements, (2) inherent mantle heterogeneity in the NW Lau mantle, unrelated to Samoa, or (3) a previously unidentified volcanic hot spot to the west of NWLSC. Our results indicate that some lavas from the NW Lau Basin have geochemical signatures similar to Samoa, but many have high $^3He/^4He$ with trace element and isotopic signatures more similar to MORB, requiring greater complexity to explain the origin of elevated $^3He/^4He$ ratios in lavas throughout the region.

Acknowledgments

[41] We thank the Master and crew of Australia's Marine National Facility Voyage SS07/08 for their skilled efforts in ensuring a productive expedition. Part of the Voyage costs was defrayed by a grant from Teck-Cominco. We thank Jianhua Wang for expert technical support in the DTM SIMS lab. We acknowledge support from NSF award OCE-0833413 to K.K., and OCE-0623208 to E.H. NSF award OCE-0644625 provided curatorial support for marine geological samples at the University of Rhode Island. We thank Stephane Escrig and Pat Castillo for detailed, thoughtful, and constructive reviews.

References

Asimow, P. D., and C. H. Langmuir (2003), The importance of water to oceanic mantle melting regimes, *Nature*, *421*, 815–820, doi:10.1038/nature01429.

Asimow, P. D., J. E. Dixon, and C. H. Langmuir (2004), A hydrous melting and fractionation model for mid-ocean ridge basalts: Application to the Mid-Atlantic Ridge near the Azores, *Geochem. Geophys. Geosyst.*, *5*, Q01E16, doi:10.1029/2003GC000568.

Bevis, M., et al. (1995), Geodetic observations of very rapid convergence and back-arc extension at the Tonga arc, *Nature*, *374*, 249–251, doi:10.1038/374249a0.

Bézos, A., S. Escrig, C. H. Langmuir, P. J. Michael, and P. D. Asimow (2009), Origins of chemical diversity of back-arc basin basalts: A segment-scale study of the Eastern Lau Spreading Center, *J. Geophys. Res.*, *114*, B06212, doi:10.1029/2008JB005924.

Conder, J. A., and D. A. Wiens (2006), Seismic structure beneath the Tonga arc and Lau back-arc basin determined from join Vp, Vp/Vs tomography, *Geochem. Geophys. Geosyst.*, *7*(3), Q03018, doi:10.1029/2005GC001113.

Conder, J. A., and D. A. Wiens (2007), Rapid mantle flow beneath the Tonga volcanic arc, *Earth Planet. Sci. Lett.*, *264*, 299–307, doi:10.1016/j.epsl.2007.10.014.

Condomines, M., K. Grønvold, P. J. Hooker, K. Muehlenbachs, R. K. O'Nions, N. Oskarsson, and E. R. Oxburgh (1983), Helium, oxygen, strontium, and neodymium isotopic relationships in Icelandic volcanics, *Earth Planet. Sci. Lett.*, *66*, 125–136, doi:10.1016/0012-821X(83)90131-0.

Cooper, L. B., T. Plank, R. J. Arculus, E. H. Hauri, P. S. Hall, and S. W. Parman (2010), High-Ca boninites from the active Tonga Arc, *J. Geophys. Res.*, *115*, B10206, doi:10.1029/2009JB006367.

Cottrell, E., and K. A. Kelley (2011), The oxidation state of Fe in MORB glasses and the oxygen fugacity of the upper mantle, *Earth Planet. Sci. Lett.*, *305*, 270–282, doi:10.1016/j.epsl.2011.03.014.

Craig, H., and J. E. Lupton (1976), Primordial neon, helium, and hydrogen in oceanic basalts, *Earth Planet. Sci. Lett.*, *31*, 369–385, doi:10.1016/0012-821X(76)90118-7.

Danyushevsky, L. V., and P. Plechov (2011), Petrolog3: Integrated software for modeling crystallization processes, *Geochem. Geophys. Geosyst.*, *12*, Q07021, doi:10.1029/2011GC003516.

Danyushevsky, L. V., T. J. Falloon, A. V. Sobolev, A. J. Crawford, M. Carroll, and R. C. Price (1993), The H_2O content of basalt glasses from southwest Pacific back-arc basins, *Earth Planet. Sci. Lett.*, *117*, 347–362, doi:10.1016/0012-821X(93)90089-R.

Dixon, J. E., and E. M. Stolper (1995), An experimental study of water and carbon dioxide solubilities in mid-ocean ridge basaltic liquids. Part II: Applications to degassing, *J. Petrol.*, *36*, 1633–1646.

Druken, K. A., C. R. Kincaid, R. A. Pockalny, R. W. Griffiths, and S. R. Hart (2009), Three-dimensional laboratory modeling of the Tonga trench and Samoan plume interaction, *Eos Trans. AGU*, *90*(52), Fall Meet. Suppl., Abstract V31D-2000.

Escrig, S., A. Bézos, S. L. Goldstein, C. H. Langmuir, and P. J. Michael (2009), Mantle source variations beneath the Eastern Lau Spreading Center and the nature of subduction components in the Lau Basin-Tonga arc system, *Geochem. Geophys. Geosyst.*, *10*, Q04014, doi:10.1029/2008GC002281.

Falloon, T. J., D. H. Green, A. L. Jacques, and J. W. Hawkins (1999), Refractory magmas in back-arc basin settings—Experimental constraints on the petrogenesis of a Lau Basin example, *J. Petrol.*, *40*, 255–277, doi:10.1093/petroj/40.2.255.

Farley, K. A., J. H. Natland, and H. Craig (1992), Binary mixing of enriched and undegasssed (primitive?) mantle components (He, Sr, Nd, Pb) in Samoan lavas, *Earth Planet. Sci. Lett.*, *111*, 183–199, doi:10.1016/0012-821X(92)90178-X.

Gill, J., and P. Whelan (1989), Early rifting of an oceanic island arc (Fiji) produced shoshonitic to tholeiitic basalts, *J. Geophys. Res.*, *94*(B4), 4561–4578, doi:10.1029/JB094iB04p04561.

Hahm, D., D. R. Hilton, P. R. Castillo, J. W. Hawkins, B. B. Hanan, and E. H. Hauri (2012), An overview of the volatile systematic of the Lau Basin–Resolving the effects of source variation, magmatic degassing and crustal contamination, *Geochim. Cosmochim. Acta*, *85*, 88–113, doi:10.1016/j.gca.2012.02.007.

Hart, S. R. (1984), A large-scale isotope anomaly in the Southern Hemisphere mantle, *Nature*, *309*, 753–757, doi:10.1038/309753a0.

Hart, S. R., E. H. Hauri, L. A. Oschmann, and J. A. Whitehead (1992), Mantle plumes and entrainment: Isotopic evidence, *Science*, *256*, 517–520, doi:10.1126/science.256.5056.517.

Hart, S. R., M. Coetzee, R. K. Workman, J. Blusztajn, K. T. M. Johnson, J. M. Sinton, B. Steinberger, and J. W. Hawkins (2004), Genesis of the Western Samoa seamount province: Age, geochemical fingerprint and tectonics, *Earth Planet. Sci. Lett.*, *227*, 37–56, doi:10.1016/j.epsl.2004.08.005.

Hawkins, J. W. (1995), Evolution of the Lau Basin: Insights from ODP Leg 135, in *Active Margins and Marginal Basins of the Western Pacific*, *Geophys. Monogr. Ser.*, vol. 88, edited by B. Taylor and J. Natland, pp. 125–173, AGU, Washington, D. C.

Hawkins, J. W., and J. T. Melchior (1985), Petrology of Mariana Trough and Lau Basin basalts, *J. Geophys. Res.*, *90*, 11,431–11,468, doi:10.1029/JB090iB13p11431.

Heyworth, Z., K. M. Knesel, S. P. Turner, and R. J. Arculus (2011), Pb-isotopic evidence for rapid trench-parallel mantle flow beneath Vanuatu, *J. Geol. Soc.*, *168*, 265–271, doi:10.1144/0016-76492010-054.

Hilton, D. R., K. Hammerschmidt, G. Loock, and H. Friedrichsen (1993), Helium and argon isotope systematic of the central Lau Basin and Valu Fa Ridge: Evidence of crust/mantle interactions in a back-arc basin, *Geochim. Cosmochim. Acta*, *57*, 2819–2841, doi:10.1016/0016-7037(93)90392-A.

Hirschmann, M. M. (2000), Mantle solidus: Experiment constraints and the effects of peridotite composition, *Geochem. Geophys. Geosyst.*, *1*(10), 1042, doi:10.1029/2000GC000070.

Jackson, M. G., S. R. Hart, A. A. P. Koppers, H. Staudigel, J. Konter, J. Blusztajn, M. D. Kurz, and J. A. Russell (2007a), The return of subducted continental crust in Samoan lavas, *Nature*, *448*, 684–687, doi:10.1038/nature06048.

Jackson, M. G., M. D. Kurz, S. R. Hart, and R. K. Workman (2007b), New Samoan lavas from Ofu Island reveal a hemispherically heterogeneous high $^3He/^4He$ mantle, *Earth Planet. Sci. Lett.*, *264*, 360–374, doi:10.1016/j.epsl.2007.09.023.

Jackson, M. G., M. D. Kurz, and S. R. Hart (2009), Helium and neon isotopes in phenocrysts from Samoan lavas: Evidence for heterogeneity in the terrestrial high $^3He/^4He$ mantle, *Earth Planet. Sci. Lett.*, *287*, 519–528, doi:10.1016/j.epsl.2009.08.039.

Jackson, M. G., S. R. Hart, J. G. Konter, A. A. P. Koppers, H. Staudigel, M. D. Kurz, J. Blusztajn, and J. M. Sinton (2010), Samoan hot spot track on a "hot spot highway": Implications for mantle plumes and a deep Samoan mantle source, *Geochem. Geophys. Geosyst.*, *11*, Q12009, doi:10.1029/2010GC003232.

Jenner, F. E., and H. C. O'Neill (2012), Analysis of 60 elements in 616 ocean floor basaltic glasses, *Geochem. Geophys. Geosyst.*, *13*, Q02005, doi:10.1029/2011GC004009.

Jenner, F. E., R. J. Arculus, J. A. Mayrogenes, N. J. Dyriw, O. Nebel, and E. H. Hauri (2012), Chalcophile element systematic in volcanic glasses from the northwestern Lau Basin, *Geochem. Geophys. Geosyst.*, *13*, Q06014, doi:10.1029/2012GC004088.

Kelley, K. A., T. Plank, T. L. Grove, E. M. Stolper, S. Newman, and E. Hauri (2006), Mantle melting as a function of water content beneath back-arc basins, *J. Geophys. Res.*, *111*, B09208, doi:10.1029/2005JB003732.

Kelley, K. A., T. Plank, S. Newman, E. M. Stolper, T. L. Grove, S. Parman, and E. H. Hauri (2010), Mantle melting as a function of water content beneath the Mariana Arc, *J. Petrol.*, *51*, 1711–1738, doi:10.1093/petrology/egq036.

Klein, E. M., and C. H. Langmuir (1987), Global correlations of ocean ridge basalt chemistry and axial depth and crustal thickness, *J. Geophys. Res.*, *92*, 8089–8115, doi:10.1029/JB092iB08p08089.

Klein, E. M., and C. H. Langmuir (1989), Global correlations of ocean ridge basalt chemistry and axial depth and crustal thickness: A reply, *J. Geophys. Res.*, *94*, 4241–4252, doi:10.1029/JB094iB04p04241.

Koppers, A. P., J. A. Russel, M. G. Jackson, J. G. Konter, H. Staudigel, and S. R. Hart (2008), Samoa reinstated as a primary hotspot trail, *Geology*, *36*, 435–438, doi:10.1130/G24630A.1.

Kurz, M. D., W. J. Jenkins, S. R. Hart, and D. Clague (1983), Helium isotope variations in volcanic rocks from Loihi Seamount and the island of Hawaii, *Earth Planet. Sci. Lett.*, *66*, 388–406, doi:10.1016/0012-821X(83)90154-1.

Kushiro, I. (1968), Compositions of magmas formed by partial zone melting of the Earth's upper mantle, *J. Geophys. Res.*, *73*, 619–634, doi:10.1029/JB073i002p00619.

Langmuir, C. H., E. M. Klein, and T. Plank (1992), Petrological systematics of mid-ocean ridge basalts: Constraints on melt generation beneath ocean ridges, in *Mantle Flow and Melt Generation at Mid-Ocean Ridges*, *Geophys. Monogr. Ser.*, vol. 71, edited by J. P. Morgan, D. K. Blackman, and J. M. Sinton, pp. 183–280, AGU, Washington, D. C.

Lee, C.-T. A., P. Luffi, T. Plank, H. Dalton, and W. P. Leeman (2009), Constraints on the depths and temperatures of basaltic magma generation on Earth and other terrestrial planets using new thermobarometers for mafic magmas, *Earth Planet. Sci. Lett.*, *279*, 20–33, doi:10.1016/j.epsl.2008.12.020.

Lupton, J. E., R. J. Arculus, R. R. Greene, L. J. Evans, and C. I. Goddard (2009), Helium isotope variations in seafloor basalts from the Northwest Lau Backarc Basin: Mapping the influence of the Samoan hotspot, *Geophys. Res. Lett.*, *36*, L17313, doi:10.1029/2009GL039468.

Lupton, J. E., R. J. Arculus, L. J. Evans, and D. Graham (2012), Mantle hotspot neon in basalts from the Northwest Lau Back-arc Basin, *Geophys. Res. Lett.*, *39*, L08308, doi:10.1029/2012GL051201.

Lux, G. (1987), The behavior of noble gases in silicate liquids: Solution, diffusion, bubbles, and surface effects, with applications to natural samples, *Geochim. Cosmochim. Acta*, *51*, 1549–1560, doi:10.1016/0016-7037(87)90336-X.

Melson, W. G., T. O'Hearn, and E. Jarosewich (2002), A data brief on the Smithsonian Abyssal Volcanic Glass Data File, *Geochem. Geophys. Geosyst.*, *3*(4), 1023, doi:10.1029/2001GC000249.

Millen, D. W., and M. W. Hamburger (1998), Seismological evidence for tearing of the Pacific plate at the northern termination of the Tonga subduction zone, *Geology*, *26*, 659–662, doi:10.1130/0091-7613(1998)026<0659:SEFTOT>2.3.CO;2.

Miller, D. M., S. L. Goldstein, and C. H. Langmuir (1994), Cerium/lead and lead isotope ratios in arc magmas and the enrichment of lead in the continents, *Nature*, *368*, 514–520, doi:10.1038/368514a0.

Montelli, R., G. Nolet, F. A. Dahlen, G. Masters, E. R. Engdahl, and S.-H. Hung (2004), Finite-frequency tomography reveals a variety of plumes in the mantle, *Science*, *303*, 338–343, doi:10.1126/science.1092485.

Newman, S., and J. B. Lowenstern (2002), VolatileCalc: A silicate melt-H_2O-CO_2 solution model written in Visual Basic for Excel, *Comput. Geosci.*, *28*(5), 597–604, doi:10.1016/S0098-3004(01)00081-4.

Niedermann, S., W. Bach, and J. Erzinger (1997), Noble gas evidence for a lower mantle component in MORBs from the southern East Pacific Rise: Decoupling of helium and neon isotope systematic, *Geochim. Cosmochim. Acta*, *61*, 2697–2715, doi:10.1016/S0016-7037(97)00102-6.

Pearce, J. A., R. J. Stern, S. H. Bloomer, and P. Fryer (2005), Geochemical mapping of the Mariana arc-basin system: Implications for the nature and distribution of subduction components, *Geochem. Geophys. Geosyst.*, *6*, Q07006, doi:10.1029/2004GC000895.

Pearce, J. A., P. D. Kempton, and J. B. Gill (2007), Hf-Nd evidence for the origin and distribution of mantle domains in the SW Pacific, *Earth Planet. Sci. Lett.*, *260*, 98–114, doi:10.1016/j.epsl.2007.05.023.

Plank, T. (2005), Constraints from thorium/lanthanum on sediment recycling at subduction zones and the evolution of the continents, *J. Petrol.*, *46*(5), 921–944, doi:10.1093/petrology/egi005.

Poreda, R. (1985), Helium-3 and deuterium in back-arc basalts: Lau Basin and the Mariana Trough, *Earth Planet. Sci. Lett.*, *73*, 244–254, doi:10.1016/0012-821X(85)90073-1.

Poreda, R. J., and H. Craig (1989), Helium isotope ratios in Circum-Pacific volcanic arcs, *Nature*, *338*, 473–478, doi:10.1038/338473a0.

Poreda, R. J., and H. Craig (1992), He and Sr isotopes in the Lau Basin mantle: Depleted and primitive mantle components, *Earth Planet. Sci. Lett.*, *113*, 487–493, doi:10.1016/0012-821X(92)90126-G.

Poreda, R., H. Craig, S. Arnorsson, and J. A. Welhan (1992), Helium isotopes in Icelandic geothermal systems I: ^{3}He, gas chemistry, and ^{13}C relations, *Geochim. Cosmochim. Acta*, *56*, 4221–4228, doi:10.1016/0016-7037(92)90262-H.

Putirka, K. (2008), Excess temperatures at ocean islands: Implications for mantle layering and convection, *Geology*, *36*, 283–286, doi:10.1130/G24615A.1.

Putirka, K., M. Perfit, F. J. Ryerson, and M. G. Jackson (2007), Ambient and excess mantle temperatures, olivine thermometry, and active vs. passive upwelling, *Chem. Geol.*, *241*, 177–206, doi:10.1016/j.chemgeo.2007.01.014.

Rison, W., and H. Craig (1983), Helium isotopes and mantle volatiles in Loihi Seamount and Hawaiian Island basalts and xenoliths, *Earth Planet. Sci. Lett.*, *66*, 407–426, doi:10.1016/0012-821X(83)90155-3.

Russo, R. M., and P. G. Silver (1994), Trench-parallel flow beneath the Nazca plate from seismic anisotropy, *Science*, *263*, 1105–1111, doi:10.1126/science.263.5150.1105.

Ryan, W. B. F., et al. (2009), Global Multi-Resolution Topography synthesis, *Geochem. Geophys. Geosyst.*, *10*, Q03014, doi:10.1029/2008GC002332.

Shaw, A. M., D. R. Hilton, C. G. Macpherson, and J. M. Sinton (2004), The CO_2-He-Ar-H_2O systematic of the Manus back-arc basin: Resolving source composition from degassing and

contamination effects, *Geochim. Cosmochim. Acta*, *68*, 1837–1855, doi:10.1016/j.gca.2003.10.015.

Shaw, A. M., E. H. Hauri, M. D. Behn, D. R. Hilton, C. G. Macpherson, and J. M. Sinton (2012), Long-term preservation of slab signatures in the mantle inferred from hydrogen isotopes, *Nat. Geosci.*, *5*, 224–228, doi:10.1038/ngeo1406.

Shen, Y., D. S. Scheirer, D. W. Forsyth, and K. C. Macdonald (1995), Trade-off in production between adjacent seamount chains near the East Pacific Rise, *J. Geophys. Res., Nature*, *373*, 140–143, doi:10.1038/373140a0.

Silver, P. G., and W. W. Chan (1991), Shear wave splitting and subcontinental mantle deformation, *J. Geophys. Res.*, *96*, 16,429–16,454, doi:10.1029/91JB00899.

Sinton, J. M., L. L. Ford, B. Chappell, and M. T. McCulloch (2003), Magma genesis and mantle heterogeneity in the Manus back-arc basin, Papua New Guinea, *J. Petrol.*, *44*(1), 159–195, doi:10.1093/petrology/44.1.159.

Sisson, T. W., and T. L. Grove (1993a), Experimental investigations of the role of H_2O in calc-alkaline differentiation and subduction zone magmatism, *Contrib. Mineral. Petrol.*, *113*, 143–166, doi:10.1007/BF00283225.

Sisson, T. W., and T. L. Grove (1993b), Temperatures and H_2O contents of low MgO high-alumina basalts, *Contrib. Mineral. Petrol.*, *113*, 167–184, doi:10.1007/BF00283226.

Smith, G. P., D. A. Wiens, K. M. Fischer, L. M. Dorman, S. C. Webb, and J. A. Hildebrand (2001), A complex pattern of mantle flow in the Lau backarc, *Science*, *292*, 713–716, doi:10.1126/science.1058763.

Spiegelman, M. (1996), Geochemical consequences of melt transport in 2-D: The sensitivity of trace elements to mantle dynamics, *Earth Planet. Sci. Lett.*, *139*, 115–132, doi:10.1016/0012-821X(96)00008-8.

Taylor, B., and F. Martinez (2003), Back-arc basin basalt systematics, *Earth Planet. Sci. Lett.*, *210*, 481–497, doi:10.1016/S0012-821X(03)00167-5.

Taylor, B., K. Zellmer, F. Martinez, and A. Goodliffe (1996), Sea-floor spreading in the Lau back-arc basin, *Earth Planet. Sci. Lett.*, *144*, 35–40, doi:10.1016/0012-821X(96)00148-3.

Tian, L., P. R. Castillo, D. R. Hilton, J. W. Hawkins, B. B. Hanan, and A. J. Pietruszka (2011), Major and trace element and Sr-Nd isotope signatures of the northern Lau Basin lavas: Implications for the composition and dynamics of the back-arc basin mantle, *J. Geophys. Res.*, *116*, B11201, doi:10.1029/2011JB008791.

Turner, S., and C. Hawkesworth (1998), Using geochemistry to map mantle flow beneath the Lau Basin, *Geology*, *26*, 1019–1022, doi:10.1130/0091-7613(1998)026<1019:UGTMMF>2.3.CO;2.

Workman, R. K., and S. R. Hart (2005), Major and trace element composition of the depleted MORB mantle (DMM), *Earth Planet. Sci. Lett.*, *231*, 53–72, doi:10.1016/j.epsl.2004.12.005.

Workman, R. K., S. R. Hart, M. G. Jackson, M. Regelous, K. A. Farley, J. Blusztajn, M. Kurz, and H. Staudigel (2004), Recycled metasomatized lithosphere as the origin of the enriched mantle II (EM2) end-member: Evidence from the Samoan volcanic chain, *Geochem. Geophys. Geosyst.*, *5*, Q04008, doi:10.1029/2003GC000623.

Workman, R. K., E. Hauri, S. R. Hart, J. Wang, and J. Blusztajn (2006), Volatile and trace elements in basaltic glasses from Samoa: Implications for water distribution in the mantle, *Earth Planet. Sci. Lett.*, *241*, 932–951, doi:10.1016/j.epsl.2005.10.028.

Wright, E., and W. M. White (1987), The origin of Samoa: New evidence from Sr, Nd, and Pb isotopes, *Earth Planet. Sci. Lett.*, *81*, 151–162, doi:10.1016/0012-821X(87)90152-X.

Zhang, S., and S. Karato (1995), Lattice preferred orientation of olivine aggregates deformed in simple shear, *Nature*, *375*, 774–777, doi:10.1038/375774a0.